J Civil Struct Health Monit (2016) 6:521–543
DOI 10.1007/s13349-016-0171-x

ORIGINAL PAPER

Enhanced particle filter for states and parameters estimation in structural health monitoring applications

Marwa Chaabane [1,2] · Majdi Mansouri[1] · Hazem Nounou [1] · Mohamed Nounou [3] · Ahmed Ben Hamida[2]

Received: 21 October 2015 / Accepted: 31 March 2016 / Published online: 2 May 2016

Abstract In this paper, an iterated square-root central difference Kalman particle filter method (ISRCDKF-PF) is used for the estimation of the state variables and model parameters of nonlinear structural systems. In the current work, we propose to extend our previous work (Mansouri et al. in J Civil Struct Health Monit 5(4):493–508, 2015) to deal with non-parametric Monte Carlo sampling-based method and propose to use an enhanced PF technique which incorporates the latest observations into a prior updating scheme using the ISRCDKF algorithm. Various conventional and state-of-the-art state estimation methods are compared for the estimation performance, namely the unscented Kalman filter (UKF), the square-root central difference Kalman filter (SRCDKF), the iterated unscented Kalman filter (IUKF), the iterated square-root central difference Kalman filter (SRCDKF), the conventional particle filter (PF), the unscented Kalman particle filter (UKF-PF), the SRCDKF-PF, the iterated unscented Kalman particle filter (IUKF-PF) and the developed ISRCDKF-PF, in two comparative studies through two examples, one using synthetic data and the other using simulated three DOF damped system data. In the first comparative study, the state variables are estimated from noisy measurements of these variables, and the comparison of the different estimation techniques is performed by computing the root mean square error (RMSE) of the state with respect to the noise-free data. In the second comparative study, both the state variables and the model parameters are simultaneously estimated, and the impact of the used measurement noise, and number of estimated states/parameters on the performances of the estimation techniques are investigated. The ISRCDKF-PF algorithm consists of a PF based on ISRCDKF to obtain a better importance proposal distribution. This proposal is able to integrate the latest observation into the state density, then it can improve the posteriori density. The results of both comparative study show that PF, UKF-PF, SRCDKF-PF, IUKF-PF and ISRCDKF-PF provide improved estimation performance over the UKF, SRCDKF, IUKF, ISRCDKF. The results also show that ISRCDKF-PF provides improved estimation performance over IUKF-PF, even with abrupt changes in estimated states, and both of them provide better accuracy than the conventional PF, UKF-PF and SRCDKF-PF. These advantages of the ISRCDKF-PF are due to the fact that it uses an optimal proposal distribution which make efficient use of the latest observation by using the ISRCDKF algorithm.

Keywords Iterated square-root central difference Kalman filter · Particle filter · State and parameter estimations · Structural health monitoring · Civil engineering infrastructure

✉ Majdi Mansouri
majdi.mansouri@qatar.tamu.edu

[1] Electrical and Computer Engineering Program, Texas A&M University at Qatar, Doha, Qatar

[2] Advanced Technologies for Medicine and Signals, National Engineering School of Sfax, Sfax, Tunisia

[3] Chemical Engineering Program, Texas A&M University at Qatar, Doha, Qatar

1 Introduction

Structural health monitoring (SHM) is an emerging field which aims at implementing damage detection and characterization strategies in various engineering structures and systems. Examples of such systems include buildings,

pipelines, highways, stadiums, and others. SHM is implemented by placing sensors on these structures to collect data that can be used to make important decisions about the condition and characteristics of these structures and systems. With the advancements in instrumentation and data acquisition techniques, monitoring of engineering structures has become cheaper, more feasible, and gained more popularity. In modal parameter estimation, the SHM system can be ill-conditioned due to uncertainties in the measurements [2, 3]. The potential errors in structural model updating combined with aleatory uncertainty in modal parameter estimation often results in inconsistencies between the real structural behavior and the finite element model predictions [4, 5]. However, in most of the published research in SHM, the ill-conditioned state and the presence of uncertainty are not considered [6]. It is also known that the dynamic responses of the structures are excitation amplitude dependent. Different levels of excitation amplitudes were reported to result in different modal damping ratios [7]. These inconsistencies in conjunction with the noisy data lead to analytical models that are sometimes far from the real behavior of the structure. This would result in wrong decisions by the SHM decision-makers and of course not contributing to the fundamental goals of the SHM process. There have been numerous SHM studies on the various uncertainty and quantification parameters such as [8–13]. Many researchers have agreed that the Bayesian approach is "relatively" strong for system identification and it is capable of addressing the uncertainty to some extent. Bayesian techniques for SHM have been researched for ambient modal identification [8, 12, 14–16], recursive filtering [17], acoustic emission-based monitoring [18, 19], distributed fiber Bragg sensors [14], optimal sensor placement [20], reliability assessment [21], seismic excitations [22], and artificial neural networks [23]. Not only in civil engineering structures, but also in aerospace and mechanical engineering structures, the emphasis in SHM research has been heavily on developing methods to better estimate the modal parameters through recorded data [2, 3]. However, there are some distinctions between the mechanical systems and civil structures for the application of some estimation methods. In addition, the SHM measurements are usually contaminated with errors hiding the important structural parameters [4, 5, 24, 25]. In an attempt to clean the contaminated data, filtering operation is conducted with Bayesian approximation techniques available in the literature. The classical Kalman filter (KF) was developed in the 1960s [26], and has been widely used in various engineering and science applications, including communications, control, machine learning, neuroscience, and many others. When the model describing the system is assumed to be linear and Gaussian, the KF provides an optimal solution [27]. It is known that the KF is computationally efficient; however, it is limited by the non-universal linear and Gaussian modeling assumptions. To relax these assumptions, the extended Kalman filter (EKF) [28], the unscented Kalman filter (UKF) [29, 30], the central difference Kalman filter (CDKF) [31], the square-root unscented Kalman filter (SRUKF) [32], the square-root central difference Kalman filter (SRCDKF) [33], the iterated unscented Kalman filter (IUKF) [34] and the iterated square-root unscented Kalman filter (ISRUKF) [1] have been developed.

The objectives of the current paper are threefold: (1) to develop an iterated square-root central difference Kalman particle filter (ISRCDKF-PF) algorithm for nonlinear and non-Gaussian estimation. In the case of the conventional PF, the latest observation is not used for the computation of the weights of the particles since the sampling distribution is equal to the prior function. This selection of the sampling distribution simplifies the evaluation, but can cause filtering divergence. In those cases where the likelihood distribution is too narrow compared to the prior one, very few particles will have significant weights. Hence, a proposal sampling distribution that takes the latest observation into account is required. In this paper, the sampling distribution is evaluated using the ISRCDKF. Hence, the ISRCDKF-PF algorithm consists of a PF based on ISRCDKF to generate the optimal importance proposal distribution. The ISRCDKF-PF algorithm allows the particle filter to incorporate the latest observations into a prior updating scheme using the estimator of the posterior distribution that matches the true posterior more closely by using the ISRCDKF algorithm. (2) To investigate the effects of practical challenges (such as measurement noise and number of estimated states/parameters) on the performances of the techniques. To study the effect of measurement noise on the estimation performances, several measurement noise levels will be considered. Then, the estimation performances of the techniques will be evaluated for different noise levels. Also, to study the effect of the number of estimated states/parameters on the estimation performances of all the techniques, the estimation performance will be studied for different numbers of estimated states and parameters. (3) To apply the proposed technique to estimate the state variables as well as the model parameters through two examples, one using synthetic data and the other using simulated three DOF damped system data. The performances of the estimation techniques will be compared to each others by computing the execution times as well as the estimation root mean square error (RMSE) with respect to the noise-free data.

The rest of the paper is organized as follows. We first discuss related work and the motivation for the need to develop the scheme in Sect. 2. In Sect. 3, the state estimation problem is presented. Then, in Sect. 4, some state

estimation methods and the developed iterated square-root central difference Kalman filter method are described. After that, in Sect. 5, the performance of the various state estimation techniques are compared for their application to estimate the state variables and model parameters in structural health monitoring system. Conclusions are presented in Sect. 6.

2 Related work

Several works based on Bayesian inference are used for state estimation in SHM systems. Mariani and Ghisi [35] used the UKF to perform the joint estimation of model parameters and state components of the softening single degree-of-freedom structural systems. While, the work in [36] showed that the UKF gives better state estimation and parameter identification than the EKF for higher degree of freedom systems and it is also robust to measurement noise levels. Eleni and Andrew [37] compared the UKF and PF methods and evaluated their efficiencies through a three-DOF damped system data.

The UKF and CDKF methods give good and similar estimation accuracies. However, in those techniques, the computation of the matrix square root of the state covariance at each time step when generating the sigma point is a costly operation. To get more numerical stability, the square root forms of the UKF and CDKF methods are numerically derived. In the SRUKF and SRCDKF methods, the square-root of the state covariance is directly propagated and updated in Cholesky factored form, using various linear algebra techniques such as the QR decomposition and the Cholesky factor updating. The SRCDKF method has equal or slightly better estimation accuracy when compared to the standard UKF, but with the benefit of having a reduced computational cost and an increased numerical stability (the covariance matrices are guaranteed to be positive definite). Otherwise, the iterative form of the UKF method gives better performance than the non-iterative one, because in the iterative schemes the observation equation is updated several times using the measurements at a single sample step, as a result the newest state estimation we get every time will be more precise. Hence, the IUKF method is more precise than the UKF method and the SRCDKF method is marginally better than the UKF method. In the same sense, ISRCDKF method is practically a computationally (potentially) more efficient of the IUKF method [34]. The ISRCDKF method employs an iterative procedure within a single measurement update step by resampling the sigma points till a termination criterion, based on the minimization of the maximum likelihood estimate, is satisfied. Furthermore, the ISRCDKF method propagates and updates the square root of the state covariance iteratively and directly in Cholesky factored form. In addition to providing reduction in the computational complexity, ISRCDKF has as increased numerical stability and better (or at least equal) performance when compared to the other algorithms. Unfortunately, for most nonlinear systems and non-Gaussian noise observations, closed-form analytic expressions of the posterior distribution of the state vector are untractable [38]. To overcome this drawback, a non-parametric Monte Carlo sampling-based method called particle filter (PF) [39, 40] has recently gained popularity. The PF approximates the posterior probability distribution by a set of weighted samples, called particles [39, 41]. PF is widely used in nonlinear and non-Gaussian systems for several filtering applications such as estimation, prediction, modeling and monitoring [42]. In case of standard PF, the latest observation is not considered for the evaluation of the weights of the particles as the importance function is taken to be equal to the prior density function [43, 44]. This choice of importance sampling function simplifies the computation but can cause filtering divergence. In cases where the likelihood function is too narrow compared to the prior function, very few particles will have significant weights [30, 45]. Hence, a better proposal distribution that takes the latest observation into account is desired in order to gain better performance [45, 46]. In the current work, we extend our previous work [1] to deal with non-parametric Monte Carlo sampling-based method and propose to use an ISRCDKF-PF technique, which consists of a PF based on ISRCDKF to generate the optimal importance proposal distribution. The ISRCDKF-PF method allows the PF to incorporate the latest observations into a prior updating scheme using ISRCDKF-based approximated posterior distribution.

3 State estimation problem

Next, we present the formulation of the state estimation problem.

3.1 Problem formulation

Consider a generic discrete-time nonlinear dynamic system described by the following dynamic state-space model (DSSM):

$$\begin{cases} x_{k+1} = f(x_k, u_k, \theta, v_k) \\ y_k = h(x_k, u_k, \theta, w_k), \end{cases} \quad (1)$$

where k is the discrete time index, $x_k \in \mathbb{R}^n$ is the state vector, $y_k \in \mathbb{R}^m$ is the measurement vector, $\theta \in \mathbb{R}^q$ is the system parameters vector, $u_k \in \mathbb{R}^p$ is the input vector, f and h are, respectively, the state and the observation functions, and $v_k \in \mathbb{R}^n$ and $w_k \in \mathbb{R}^m$ are mutually independent i.i.d noise processes.

In this paper, the input vector u_k is assumed to be known. However, the vector of system parameters θ is taken to be unknown and it will be jointly estimated with the state vector. For the sake of computational expediency, we assume that the unknown system parameter vector evolves artificially in time according to a random walk as follows:

$$\theta_k = \theta_{k-1} + \eta_{k-1}, \tag{2}$$

where r_{k-1} is a sequence of i.i.d zero-mean Gaussian random variables. In such estimation problems, the state vector and the system parameter vector are usually concatenated into a single higher-dimensional joint state vector, $z_k \in \mathbb{R}^{n+q}$, defined as:

$$z_k = \begin{bmatrix} x_k^T & \theta_k^T \end{bmatrix}^T \tag{3}$$

Using the augmented state vector, the process equation of the DSSM (1) can be expanded to:

$$z_{k+1} = \begin{bmatrix} x_{k+1} \\ \theta_{k+1} \end{bmatrix} = \begin{bmatrix} f(x_k, u_k, v_k, \theta_k) \\ \theta_k + \eta_k \end{bmatrix} \tag{4}$$

Also, defining the augmented noise vector as $\tilde{w}_k = \begin{bmatrix} v_k^T & \eta_k^T \end{bmatrix}^T$, the DSSM (1) can be written as:

$$\begin{cases} z_{k+1} = f(z_k, u_k, \tilde{w}_k) \\ y_k = l(z_k, u_k, v_k), \end{cases} \tag{5}$$

where f and l are differentiable nonlinear functions.

4 Description of state estimation methods

4.1 Square-root central difference Kalman filter (SRCDKF) method

For nonlinear system, the EKF recursively calculates the mean and the covariance $\mathbf{P}_k$ of the random variable, while the UKF calculates the matrix square-root $\mathbf{S}_k\mathbf{S}_k^T = \mathbf{P}_k$, at each time step. However, the SRCDKF directly propagate the square-root covariance matrix $\mathbf{S}_k$ avoiding the computational complexity to refactorize at each time step [32]. The SRCDKF firstly initializes the mean of the state vector and the square root of it covariance.

$$\hat{z}_0 = E[z_0], \tag{6}$$

and

$$\mathbf{S}_0 = \text{chol}\left\{E\left[(z_0 - \hat{z}_0)(z_0 - \hat{z}_0)'\right]\right\}. \tag{7}$$

The Cholesky factorization produces an upper triangular matrix from the decomposition of a symmetric, positive-definite matrix into the product of a lower-triangular matrix and its transpose. This new matrix is utilized directly to generate the sigma points:

$$\mathbf{\Psi}_{k-1} = [\hat{z}_{k-1} \quad \hat{z}_{k-1} + h\mathbf{S}_{k-1} \quad \hat{z}_{k-1} - h\mathbf{S}_{k-1}], \tag{8}$$

where $\hat{z}_{k-1} = [\hat{z}_{k-1} \quad \bar{v}]$, $\mathbf{S}_{k-1} = \text{diag}[\mathbf{S}_{k-1} \quad \mathbf{S}_v]$ and h is a scaling parameter equal to the kurtosis of the prior random variable. The optimal value of h for Gaussian random variables is $h = \sqrt{3}$.

Next, the sigma points are propagated through the nonlinear process system to predict the current attitude based on each sigma point.

$$\mathbf{\Psi}_{k|k-1} = f[\mathbf{\Psi}_{k-1}]. \tag{9}$$

Then the state mean and square-root covariance are estimated from the transformed sigma points using,

$$\hat{z}_k^- = \sum_{i=0}^{2L} W_i^{(m)} \mathbf{\Psi}_{i,k|k-1}, \tag{10}$$

and

$$\mathbf{S}_k^- = qr\left\{\left[\sqrt{W_1^{(c1)}}(\mathbf{\Psi}_{1:L,k|k-1} - \mathbf{\Psi}_{L+1:2L,k|k-1}) \quad \sqrt{W_1^{(c2)}}(\mathbf{\Psi}_{1:L,k|k-1} + \mathbf{\Psi}_{L+1:2L,k|k-1} - 2\mathbf{\Psi}_{0,k|k-1})\right]\right\}, \tag{11}$$

where $W_i^{(c1)} = \frac{1}{4h^2}$, $W_i^{(c2)} = \frac{h^2-1}{4h^4}$, $W_0^{(m)} = \frac{h^2-L}{h^2}$, $W_i^{(m)} = \frac{1}{2h^2}$.

The next step, the sigma-point for measurement update is generated as,

$$\mathbf{\Psi}_{k|k-1} = \left[\hat{z}_{k|k-1} \quad \hat{z}_{k|k-1} + h\mathbf{S}_{k|k-1} \quad \hat{z}_{k|k-1} - h\mathbf{S}_{k|k-1}\right], \tag{12}$$

where $\hat{z}_{k|k-1} = \left[\hat{z}_{k|k-1} \quad \bar{w}\right]$, $\mathbf{S}_{k|k-1} = \text{diag}\left[\mathbf{S}_{k|k-1} \quad \mathbf{S}_w\right]$.

The measurements sigma points are propagated through the measurement model:

$$Y_{k|k-1} = h\left[\mathbf{\Psi}_{k|k-1}\right]. \tag{13}$$

To predict the measurements, the expected measurement $\hat{y}_k^-$ and square-root covariance of $\tilde{y}_k = y_k - \hat{y}_k^-$ (called the innovation) are calculated as:

$$\hat{y}_k^- = \sum_{i=0}^{2L} W_i^{(m)} Y_{i,j}. \tag{14}$$

$$\tilde{y}_k = y_k - \hat{y}_k^-, \tag{15}$$

$$\mathbf{S}_{\tilde{y}_k} = qr\left\{\left[\sqrt{W_1^{(c1)}}(Y_{1:L,j} - Y_{L+1:2L,j}) \quad \sqrt{W_1^{(c2)}}(Y_{1:L,j} + Y_{L+1:2L,j} - 2Y_{0,j})\right]\right\}. \tag{16}$$

In order to find out how much to adjust the predicted state mean and covariance based on the actual measurement, the Kalman gain matrix $\mathbf{K}_k$ is calculated as follows:

$$\mathbf{P}_{z_k y_k} = W_i^{(c1)} S_k^- [Y_{1:L,j} - Y_{L+1:2L,j}]^T. \tag{17}$$

$$\mathbf{K}_{k,j} = \mathbf{P}_{z_k y_k} / \mathbf{S}_k^T / \mathbf{S}_{\bar{\mathbf{y}}_\mathbf{k}}. \tag{18}$$

Then, updated state mean and covariance are expressed using the actual measurement and the Kalman gain matrix as:

$$\hat{z}_k = \hat{z}_k^- + \mathbf{K}_k(y_k - \hat{y}_k^-). \tag{19}$$

$$\mathbf{U} = \mathbf{K}_k \mathbf{S}_{\bar{y}_k}. \tag{20}$$

$$\mathbf{S}_k = cholupdate\{\mathbf{S}_k^-, \mathbf{U}, -1\}, \tag{21}$$

where $\mathbf{S}_v = \sqrt{\mathbf{R}^v}$ is the square root of the process noise covariance matrix, $\mathbf{S}_w = \sqrt{\mathbf{R}^w}$ is the square root of the measurement noise covariance matrix, chol - is Cholesky method of matrix factorization, qr is QR matrix decomposition and cholupdate is a Cholesky factor updating.

The benefit of the ISRCDKF method lies in its ability to provide accuracy-related advantages over other estimation methods since it re-linearizes the measurement equation by iterating an approximate maximum a posteriori estimate around the updated state, instead of relying on the predicted state. Next, ISRCDKF is presented.

4.2 Iterated square-root central difference Kalman filter (ISRCDKF) method

With the success of IUKF method development [34] and the superiority of SRCDKF, an improved performance would be expected if the iterates are implemented in SRCDKF. With the potential problems experienced with the IUKF method, precaution should be taken for effective performance of the iterated filter [47]. The development of the ISRCDKF method is due to the need to overcome this issue, utilizing a different iteration strategy.

In the ISRCDKF method, we apply the iterations on the process of measurement update where the updated state estimation is calculated using the predicted state and the observation. Instead of relying on the predicted state, the observation equation is re-linearized over times by iterating an approximate maximum a posteriori estimate, so the state estimate will be more accurate.

In the iterated measurement update step of the SRCDKF approach, the new sigma points are generated at each iteration from the latest estimation of the posterior state distribution.

The square-root central difference approach is applied again with the state estimation $\hat{z}_k$ which will be expressed as z_j in the iteration and indicates the state estimation in the jth iteration. Then, the state estimate is performed by the measurement value. This is how the ISRCDKF works.

After the estimated mean $\hat{z_k}^-$ and the covariance matrix S_k^- are obtained, z_j is obtained by the filtering algorithm. The sampling points are re-generated based on z_j and S_k^- by the following equation:

$$\mathbf{\Psi}_j = \begin{bmatrix} z_j & z_j + h\mathbf{S}_k^- & z_j - h\mathbf{S}_k^- \end{bmatrix} \tag{22}$$

The new generated sample points pass through the measurement equation:

$$Y_j = h[\mathbf{\Psi}_j], \tag{23}$$

$$\hat{y}_j^- = \sum_{i=0}^{2L} W_i^{(m)} Y_{i,j}, \tag{24}$$

$$\tilde{y}_k = y_k - \hat{y}_k^-, \tag{25}$$

$$\mathbf{S}_{\tilde{y}_k} = QR\left\{\left[\sqrt{W_1^{(c1)}}(Y_{1:L,j} - Y_{L+1:2L,j})\sqrt{W_1^{(c2)}}(Y_{1:L,j} + Y_{L+1:2L,j} - 2Y_{0,j})\right]\right\}, \tag{26}$$

$$\mathbf{P}_{z_k y_k} = W_i^{(c1)} S_k^- [Y_{1:L,j} - Y_{L+1:2L,j}]^T. \tag{27}$$

Then, the Kalman gain K_k is be re-calculated:

$$\mathbf{K}_{k,j} = \mathbf{P}_{z_k y_k} / \mathbf{S}_k^T / \mathbf{S}_{\bar{\mathbf{y}}_\mathbf{k}}. \tag{28}$$

Next, the state estimate update is improved using y_j instead of $\hat{y}_k$:

$$\hat{z}_k = \hat{z}_k^- + \mathbf{K}_k(y_k - \hat{y}_j^-). \tag{29}$$

Finally, the covariance matrix is re-calculated:

$$\mathbf{U} = \mathbf{K}_k \mathbf{S}_{\bar{y}_k}, \tag{30}$$

Algorithm 1: Iterated Square Root Central Difference Kalman Filter algorithm

Initialization:

$\hat{z}_0 = E[z_0]$

$\mathbf{S}_0 = chol\{E[(z_0 - \hat{z}_0)(z_0 - \hat{z}_0)']\}$.

Calculating sigma points for time update:

$\Psi_{k-1} = [\hat{z}_{k-1} \quad \hat{z}_{k-1} + h\mathbf{S}_{k-1} \quad \hat{z}_{k-1} - h\mathbf{S}_{k-1}]$,

$\Psi_{k|k-1} = f[\Psi_{k-1}]$.

Time update:

$\hat{z}_k^- = \sum_{i=0}^{2L} W_i^{(m)} \Psi_{i,k|k-1}$,

$S_k^- = qr \quad \sqrt{W_1^{(c1)}}(\Psi_{1:L,k|k-1} - \Psi_{L+1:2L,k|k-1})\sqrt{W_1^{(c2)}}(\Psi_{1:L,k|k-1} + \Psi_{L+1:2L,k|k-1} - 2\Psi_{0,k|k-1})$,

Calculating sigma-point for measurement update:

$\Psi_{k|k-1} = \quad \hat{z}_{k|k-1} \quad \hat{z}_{k|k-1} + h\mathbf{S}_{k|k-1} \quad \hat{z}_{k|k-1} - h\mathbf{S}_{k|k-1}$.

Measurement update:

$z_0 = \hat{z}_k^-$,

for $i = 0, \ldots, m$ **do**

$\Psi_j = \left[z_j \quad z_j + h\mathbf{S}_k^- \quad z_j - h\mathbf{S}_k^-\right]$,

$Y_j = h[\Psi_j]$,

$\hat{y}_j^- = \sum_{i=0}^{2L} W_i^{(m)} Y_{i,j}$,

$\mathbf{S}_{\tilde{y}_k} = QR \quad \sqrt{W_1^{(c1)}}(Y_{1:L,j} - Y_{L+1:2L,j})\sqrt{W_1^{(c2)}}(Y_{1:L,j} + Y_{L+1:2L,j} - 2Y_{0,j})$,

$\mathbf{P}_{z_k y_k} = W_i^{(c1)} S_k^- [Y_{1:L,j} - Y_{L+1:2L,j}]^T$,

$\mathbf{K}_{k,j} = \mathbf{P}_{z_k y_k} / \mathbf{S}_k^T / \mathbf{S}_{\tilde{y}_j}$,

$\hat{z}_{j+1} = \hat{z}_k^- + \mathbf{K}_{k,j}(y_k - \hat{y}_j^-)$,

$\mathbf{U} = \mathbf{K}_{k,j}\mathbf{S}_{\tilde{y}_k}$,

$\mathbf{S}_k = cholupdate\left\{\mathbf{S}_k^-, \mathbf{U}, -1\right\}$.

end

$\mathbf{U} = \mathbf{K}_{k,m}\mathbf{S}_{\tilde{y}_k}$,

$\mathbf{S}_k = cholupdate\left\{\mathbf{S}_k^-, \mathbf{U}, -1\right\}$.

Return the augmented state estimation $\widehat{z}_k$.

$$\mathbf{S}_k = cholupdate\left\{\mathbf{S}_k^-, \mathbf{U}, -1\right\}. \tag{31}$$

The algorithm of the ISRCDKF method can be summarized in Algorithm 1.

4.3 Conventional particle filter (PF) method

A particle filter is an implementation of a recursive Bayesian estimator [30, 48]. Bayesian estimation relies on computing the posterior $p(z_k|y_{0:k})$, which is the density function of the unobserved state vector, z_k, given the sequence of the observed data $y_{0:k} \equiv \{y_0, y_2, \ldots, y_k\}$. In a Bayesian context, the task of state estimation can be formulated as recursively calculating the predictive distribution $p(z_k|y_{0:k-1})$ and the filtering distribution $p(z_k|y_{0:k})$ as follows [30],

$$\begin{aligned} p(z_k|y_{0:k-1}) &= \int_{\mathbb{R}^n} p(z_k|z_{k-1})p(z_{k-1}|y_{0:k-1})\mathrm{d}z_{k-1}, \\ p(z_k|y_{0:k}) &= \frac{p(y_k|z_k)p(z_k|y_{0:k-1})}{p(y_k|y_{0:k-1})}, \end{aligned} \tag{32}$$

where the normalizing constant $p(y_k|y_{0:k-1}) = \int_{\mathbb{R}^z} p(y_k|z_k)\, p(z_k|y_{0:k-1})\mathrm{d}z_k$.

The nonlinear nature of the system model leads to intractable integrals when evaluating the marginal state distribution, $p(z_k|z_{k-1})$. Therefore, Monte Carlo approximation is utilized, where the joint posterior distribution, $p(z_{0:k}|y_{0:k})$, is approximated by the point-mass distribution of a set of weighted samples (particles) $\{z_{0:k}^{(i)}, \ell_k^{(i)}\}_{i=0}^N$, i.e., [30, 49]:

$$\hat{p}_N(z_{0:k}|y_{0:k}) = \sum_{i=0}^{N} \ell_k^{(i)} \delta_{z_{0:k}^{(i)}}(\mathrm{d}\, z_{0:k}) / \sum_{i=0}^{N} \ell_k^{(i)}, \tag{33}$$

where $\delta_{z_{0:k}^{(i)}}(\mathrm{d}\, z_{0:k})$ denotes the Dirac function, $\ell_k^{(i)}$ are the corresponding importance weights and N is the total number of particles. Based on the same set of particles, the marginal posterior probability of interest, $p(z_k|y_{0:k})$, can also be approximated as follows [30, 42]:

$$\hat{p_N}(z_k|y_{0:k}) = \sum_{i=0}^{N} \ell_k^{(i)} \delta_{z_k^{(i)}}(\mathrm{d}\, z_k) / \sum_{i=0}^{N} \ell_k^{(i)}. \tag{34}$$

In this Bayesian importance sampling (IS) approach, the particles $\{z_{0:k}^{(i)}\}_{i=0}^N$ are sampled from the following distribution (called also Importance density) [42],

$$p(z_{0:k}|y_{0:k}) = p(z_k|z_{k-1}) = \int \mathcal{N}(z_k|\mu_k, \lambda_k)p(\mu_k, \lambda_k|z_{k-1})\mathrm{d}\mu_k\mathrm{d}\lambda_k, \quad (35)$$

where μ_k defines the expectation of the state z_k and λ_k defines the covariance matrix of the state z_k.

$$\hat{N}_{\text{eff}} = \frac{1}{\sum_{i=0}^{N}(\ell_k^{(i)})^2}, \quad (38)$$

where $\ell_k^{(i)}$ are the normalized weights obtained using (37).

The conventional PF algorithm for state/parameter estimation is summarized in Algorithm 2.

Algorithm 2: Conventional particle filtering algorithm

Input: y_k

Output: $\widehat{z}_k$

for $i = 0, 1, \ldots, N$ **do**

Importance sampling step:

Sample $\widetilde{z}_k^{(i)} \sim p(z_k^{(i)}|z_{0:k-1}^{(i)}, y_{0:k})$, according the equation (35), and set $\widetilde{z}_{0:k}^{(i)} = (z_{0:k-1}^{(i)}, z_k^{(i)})$;

Compute the approximated joint distribution, $\hat{p}_N(z_{0:k}|y_{0:k})$, using equation (33);

Evaluate importance weights using equation (37);

Normalize importance weights:

$$\widetilde{\ell}_k^{(i)} = \frac{\ell_k^{(i)}}{\sum_{j=1}^{N}(\ell_k^{(j)})}$$

Selection step:

if $N_{eff} = \frac{1}{\sum_{i=0}^{N}(\ell_k^{(i)})^2} < N_{threshold}$ **then**

Resample with replacement N particles $\{z_{0:k}^{(i)}\}_{i=0}^{N}$ from the set $\{\widetilde{z}_{0:k}^{(i)}\}_{i=0}^{N}$ according to the normalized importance weights, $\ell_k^{(i)} = \widetilde{\ell}_k^{(i)}$;

Compute the estimated state using equation (36);

end

end

Return the augmented state estimation $\widehat{z}_k$.

Resampling is performed whenever the effective sample size N_{eff} drops below a certain threshold $N_{\text{threshold}}$, where a smaller N_{eff} means a larger variance for the weights, hence more degeneracy.

Then, the estimate of the augmented state $\widehat{z}_k$ can be approximated by a Monte Carlo scheme as follows [49]:

$$\widehat{z}_k = \sum_{i=0}^{N} \ell_k^{(i)} z_k^{(i)}, \quad (36)$$

where $\ell_k^{(i)}$ is given by [49]:

$$\ell_k^{(i)} \propto \frac{p(y_{0:k}|z_{0:k}^{(i)})p(z_{0:k}^{(i)})}{p(z_{0:k}^{(i)}|y_{0:k})}. \quad (37)$$

A common problem with the sequential importance sampling-based particle filter is the degeneracy phenomenon. This degeneracy implies that a large computational effort is devoted to updating particles whose contribution to the approximation of $p(z_k|y_{0:k})$ is almost zero. A suitable measure of degeneracy of the algorithm is the estimate effective sample size $\hat{N}_{eff}$, which is introduced in [48] and [50], and is defined as,

Particle filtering suffers from one major drawback. Its efficient implementation requires the ability to sample from $p(z_k|z_{k-1})$, which does not take into account the current observed data, y_k, and thus many particles can be wasted in low likelihood (sparse) areas [30]. This issue is addressed by the iterated square-root central difference Kalman particle filter, which is described in next Section.

4.4 Iterated square-root central difference Kalman particle filter (ISRCDKF-PF) Method

The choice of optimal proposal function is one of the most critical design issues in importance sampling schemes. In [49], the optimal proposal distribution $\hat{p}(z_k|z_{0:k-1}, y_{0:k})$ is obtained by minimizing the variance of the importance weights given the states $z_{0:k-1}$ and the observations data $y_{0:k}$. This selection has also been studied by other researchers. However, this optimal choice suffers from one major drawback. The particles are sampled from the prior density $p(z_k|z_{0:k-1})$ and the integral over the new state need to be computed. In the general case, closed-form analytic expression of the posterior distribution of the state is untractable [38]. Therefore, the distribution $p(z_k|z_{0:k-1})$ is

the most popular choice of proposal distribution. One of the advantages of PF is its simplicity in sampling from the prior functions $p(z_k|z_{0:k-1})$ and the evaluation of weights $\ell_k^{(i)}$ (as presented in the previous section) [38]. However, the latest observation is not considered for the computation of the weights of the particles as the importance density is taken to be equal to the prior density [43]. The transition prior $p(z_k|z_{0:k-1})$ does not take into account the current observation data y_k, and many particles can be wasted in low likelihood areas. This choice of importance sampling function simplifies the computational complexity but can cause filtering divergence [30, 45]. In cases where the likelihood density is too narrow as compared to the prior function, very few particles will have considerable weights. Therefore, the distribution $p(z_k|z_{0:k-1})$ is the most popular choice of proposal distribution. Although the ISRCDKF-PF moves the prior toward the likelihood, which due to creating a better proposal distribution, this is done by generating an optimal importance proposal distribution by using ISRCDKF method (as presented in Sect. 4.2). Hence, the ISRCDKF-PF algorithm consists of a PF based on ISRCDKF to generate the optimal importance proposal distribution. The proposal distribution integrates the latest observation into system state transition density.

The developed ISRCDKF-PF algorithm can be summarized in Algorithm 3.

Algorithm 3: Iterated square root central difference Kalman particle filter algorithm

Input: y_k

Output: $\widehat{z}_k$

Initialization at time k=0

for $i = 0, 1, \ldots, N$ **do**

  Draw the particles $z_0^{(i)}$ from the prior $p(z_0)$;

end

for $k = 1, 2, \ldots$ **do**

  for $i = 0, 1, 2 \ldots$ **do**

    Importance sampling step:

    - Update the particles with ISRCDKF to generate the important density function $[\hat{z}_k^{(i)}, S_k^{(i)}]$=ISRCDKF$(z_{k-1}^{(i)}, S_{k-1}^{(i)}, y_k)$
    - Sample the particles $\widetilde{z}_k^{(i)} \sim p(z_k^{(i)}|z_{0:k-1}^{(i)}, y_{1:k}) = \mathcal{N}(z_k, \hat{z}_k^{(i)}, S_k^{(i)})$,
    - Evaluate importance weights $\ell_k^{(i)} \propto \ell_{k-1}^{(i)} \frac{p(y_{0:k}|\widetilde{z}_{0:k}^{(i)}) p(\widetilde{z}_{0:k}^{(i)})}{p(\widetilde{z}_{0:k}^{(i)}|y_{0:k})}$
    - Normalize importance weights: $\widetilde{\ell}_k^{(i)} = \frac{\ell_k^{(i)}}{\sum_{j=1}^{N}(\ell_k^{(j)})}$

    Selection step:

    Compute $N_{eff} = \frac{1}{\sum_{i=0}^{N}(\ell_k^{(i)})^2}$

    if $N_{eff} < N_{threshold}$ **then**

      Re-sample the particles: Suppress particles with low weights and duplicate particles with large weights.

      The particles are denoted $\widetilde{z}_k^{(i)}$ according to the weights, $\widetilde{\ell}_k^{(i)} = \frac{1}{N}$;

    end

  end

end

Return the augmented state estimation $\widehat{z}_k$.

5 Simulation results

5.1 State and parameter estimations for a scalar nonlinear system

Next, the estimation performance is evaluated and the developed ISRCDKF-PF method is compared to UKF, SRCDKF, IUKF, ISRCDKF, PF, UKF-PF, SRCDKF-PF and IUKF-PF methods through a scalar nonlinear system (40). The purpose of this section is to estimate the state variable x_k and the model parameter ϕ_1. The equations representing the system can be written as follows:

$$x_k = \phi_1 x_{k-1} + 1 + \sin(\omega\pi(k-1)) + v_k, \tag{39}$$

where v_k is a $N(v_k; 0, 10^{-4})$ Gaussian distribution modeling the process noise, and ω = 0.04 and ϕ_1 = 0.5 are scalar parameters. The non-stationary observation model is given by:

$$y_k = \begin{cases} \phi_2 x_k^2 + n_k & \text{for} \quad k <= 30 \\ \phi_3 x_k - 2 + n_k & \text{for} \quad k > 30, \end{cases} \tag{40}$$

where ϕ_2 = 0.2 and ϕ_3 = 0.5. The observation noise, n_k, is drawn from a Gaussian distribution $\mathcal{N}(n_k; 0, 10^{-4})$.

For all simulations, the number of sigma points is fixed to 5 for all the techniques ($L = 2$) and the particle filters use 500 particles. The initial values of the augmented state vector are fixed to $z(0) = [x_0 \quad \theta_0] = [1 \quad 0.1]$.

5.1.1 *Comparative study 1: estimation of state variables from noisy measurements*

Here, we compare the estimation accuracy of UKF, SRCDKF, IUKF, ISRCDKF, PF, UKF-PF, SRCDKF-PF, IUKF-PF and ISRCDKF-PF methods when they are utilized to estimate the state variable of the system model. Hence, it is considered that the state vector to be estimated is $z_k = x_k$, and the model parameter, ϕ_1, is assumed to be known.

The simulation results for the estimation of state variable x_k using UKF, SRCDKF, IUKF, ISRCDKF, PF, UKF-PF, SRCDKF-PF, IUKF-PF and ISRCDKF-PF methods are shown in Figs. 1 and 2, respectively. Also, the performance comparison of the state estimation techniques in terms of RMSE is presented in Table 1. It is easily observed from Figs. 1 and 2 as well as Table 1 that UKF is outperformed by the alternative techniques. The results also show that the ISRCDKF-PF method achieves a better accuracy than the other methods.

5.1.2 *Comparative study 2: simultaneous estimation of state variables and model parameters*

The estimation of the state variables and parameters were performed using the state estimation techniques, UKF, SRCDKF, IUKF, ISRCDKF, PF, UKF-PF, SRCDKF-PF, IUKF-PF and ISRCDKF-PF. The estimation results for the model parameters using these estimation techniques are shown in Figs. 3, and 4, respectively.

It can be seen from the results presented in Figs. 3 and 4 that the IUKF-PF, SRCDKF-PF and ISRCDKF-PF methods outperform the UKF-PF method, and that the ISRCDKF-PF shows relative improvement over all other techniques. These results confirm the results obtained in the first comparative study, where only the state variable is estimated. The advantages of the ISRCDKF-PF over the other techniques can also be seen through their abilities to estimate the model parameters. For example, UKF, IUKF, SRCDKF and ISRCDKF could took longer to estimate a model parameters (see Figs. 3, 4).

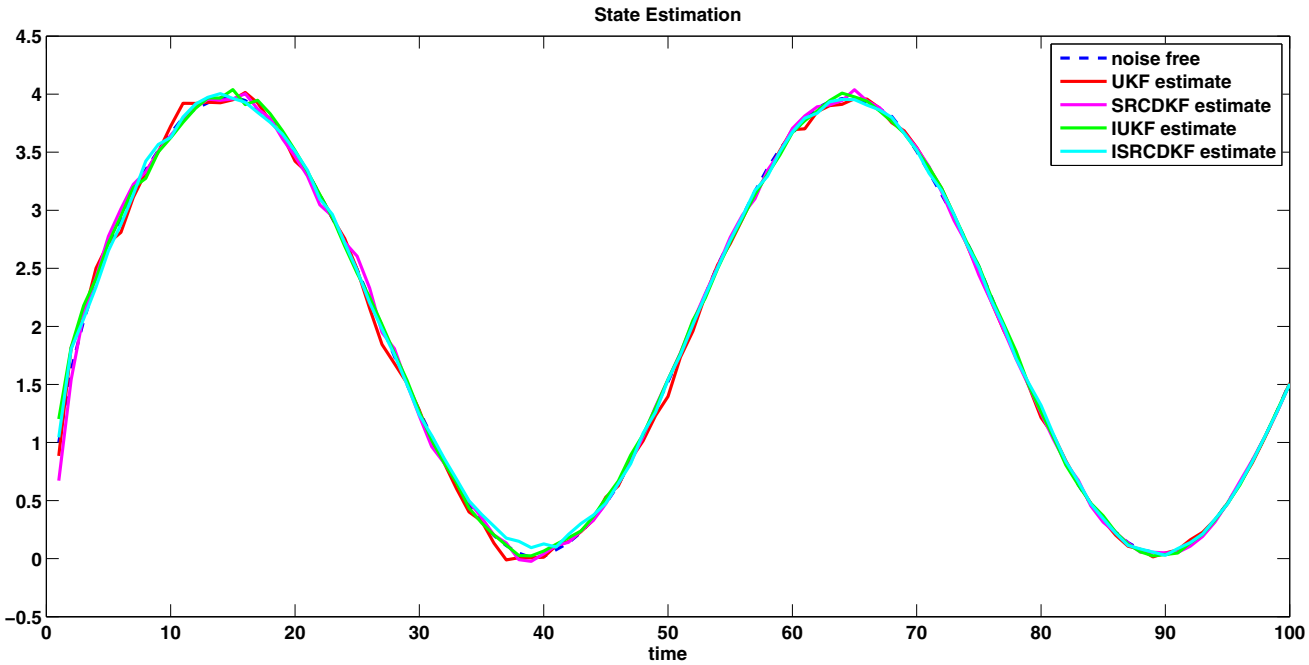

Fig. 1 Estimation of state variable using various state estimation techniques (UKF, SRCDKF, IUKF, ISRCDKF)

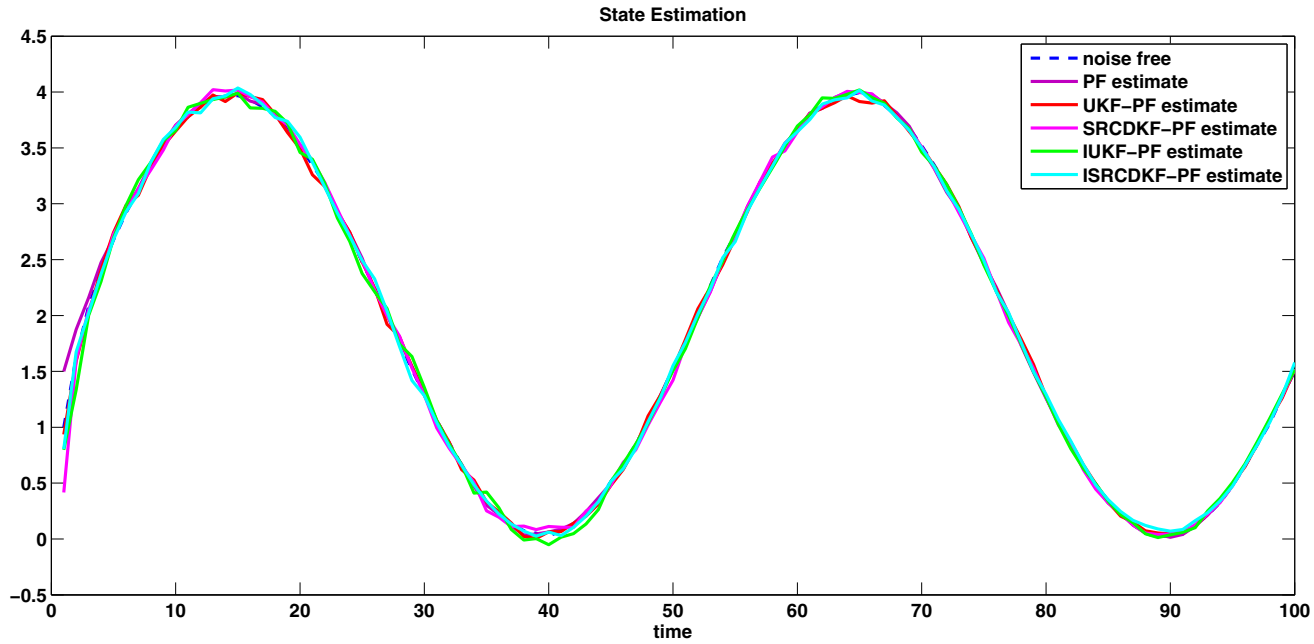

Fig. 2 Estimation of state variable using various state estimation techniques (PF, UKF-PF, IUKF-PF, SRCDKF-PF, ISRCDKF-PF)

Table 1 Comparison of state estimation techniques

Technique	x_k (RMSE)	Technique	x_k (RMSE)
		PF	0.0344
UKF	0.0378	UKF-PF	0.0312
SRCDKF	0.0374	SRCDKF-PF	0.0308
IUKF	0.0367	IUKF-PF	0.0294
ISRCDKF	0.0360	ISRCDKF-PF	0.0288

5.1.3 Effect of number of state and parameter to estimate on the estimation RMSE

To study the effect of the number of states and parameters to be estimated on the estimation performances of UKF, SRCDKF, IUKF, ISRCDKF, PF, UKF-PF, SRCDKF-PF, IUKF-PF and ISRCDKF-PF, the estimation performance is analyzed for different numbers of estimated states and

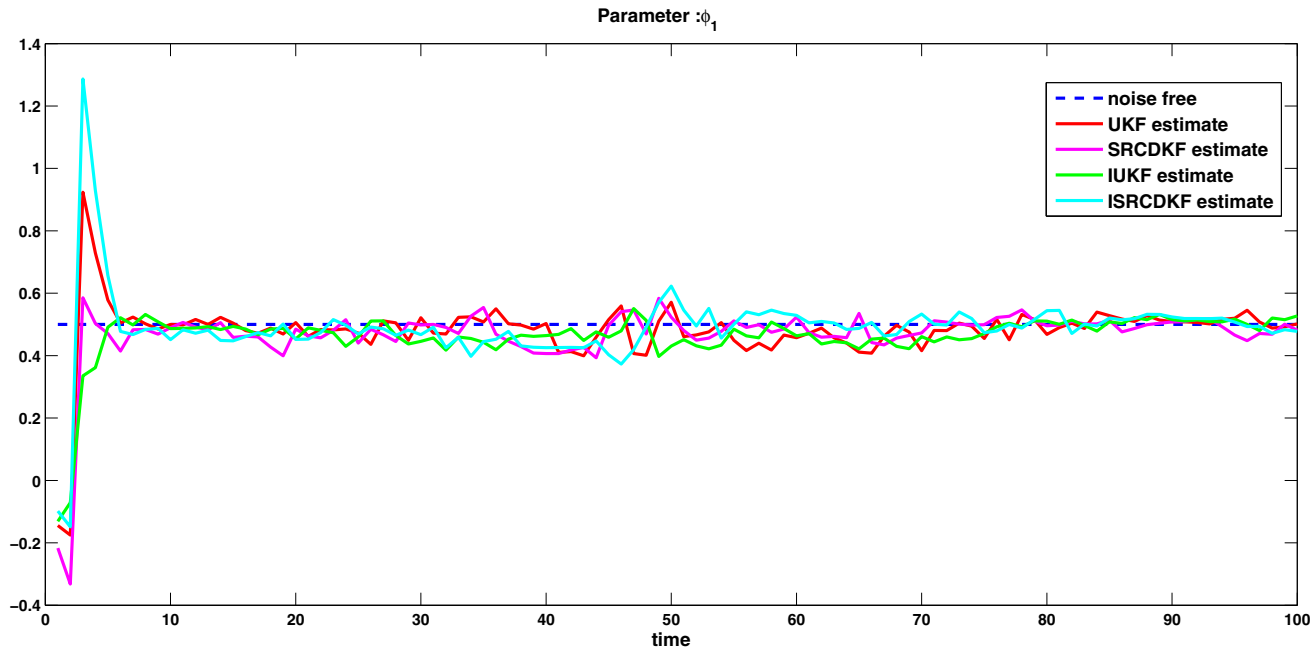

Fig. 3 Estimation of the model parameter (ϕ_1) using UKF, SRCDKF, IUKF and ISRCDKF

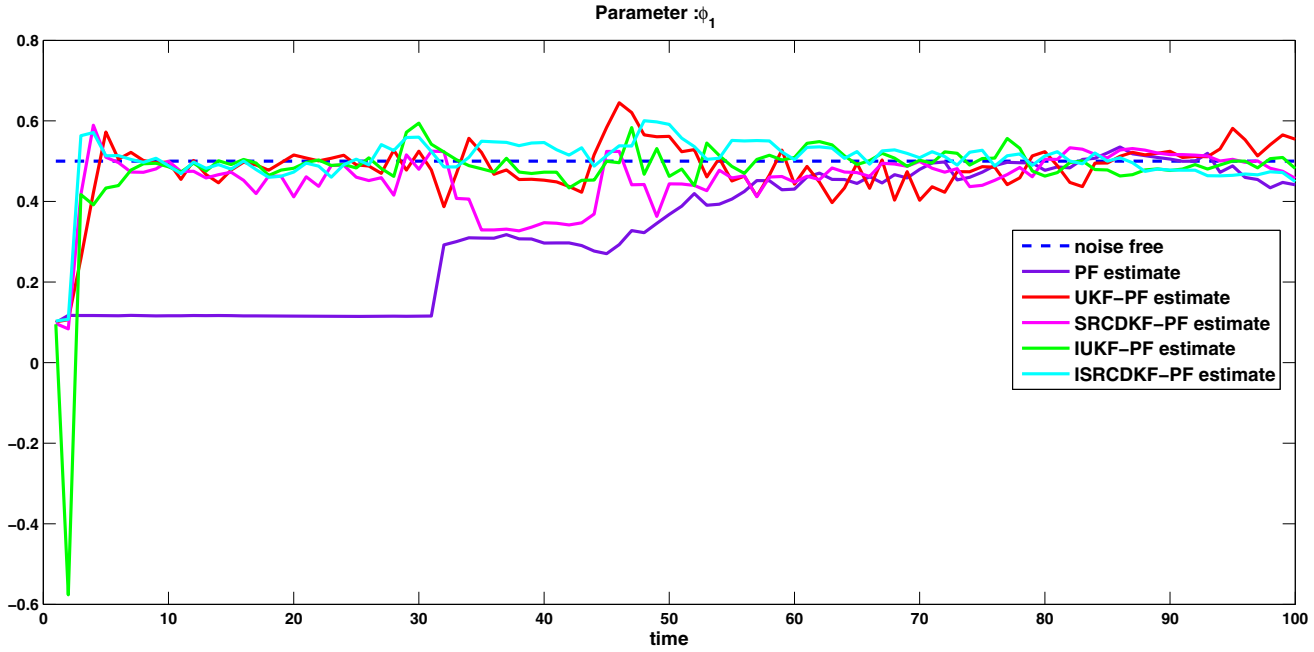

Fig. 4 Estimation of the model parameter (ϕ_1) using UKF-PF, IUKF-PF, SRCDKF-PF and ISRCDKF-PF

Table 2 Root mean square errors of estimated state variables and mean of estimated parameter

Technique	x_k (RMSE)	ϕ_1 (mean)	Technique	x_k (RMSE)	ϕ_1 (mean)
			PF	0.4310	0.4166
UKF	0.0858	0.4838	UKF-PF	0.0664	0.4932
SRCDKF	0.0850	0.4845	SRCDKF-PF	0.0655	0.4936
IUKF	0.0790	0.4895	IUKF-PF	0.0619	0.4951
ISRCDKF	0.0784	0.4902	ISRCDKF-PF	0.0610	0.4958

parameters. The estimation of the state variable and parameter is performed using the techniques, and the simulation results for the state variable and the model parameters are shown in Table 2. Table 2 compares the estimation root mean square errors for the state variable x_k (with respect to the noise-free data) and the mean of the estimated parameter ϕ_1 (true value of ϕ_1) at steady state (i.e., after convergence of the parameter) using UKF, SRCDKF, IUKF, ISRCDKF, PF, UKF-PF, SRCDKF-PF, IUKF-PF and ISRCDKF-PF, respectively.

The results also show that the number of states and parameters to estimate affects the estimation accuracy of the state variable. In other words, the estimation RMSE of x_k increases from the first comparative study where only the state variable x_k is estimated to the case where the state variable x_k and one parameter ϕ_1 are estimated.

For example, the RMSEs obtained using ISRCDKF-PF for x_k in the first comparative study and the second comparative study are 0.0288 and 0.0610, respectively, which increase as the number of estimated parameters increases (see Table 2). This observation is valid for the other state estimation techniques.

5.2 State and parameter estimations for three degree of freedom spring–mass–dashpot system

Here, we consider the example of sensor heterogeneity arising from the fact that both acceleration and displacement are measured at various locations of the structural system. The availability of non-collocated data might often arise in the identification of systems where the displacement data may be provided through global positioning systems. The performance of developed ISRCDKF-PF is evaluated through the example of a three degree-of-freedom system, involving a Bouc–Wen hysteretic component, where the availability of displacement and acceleration

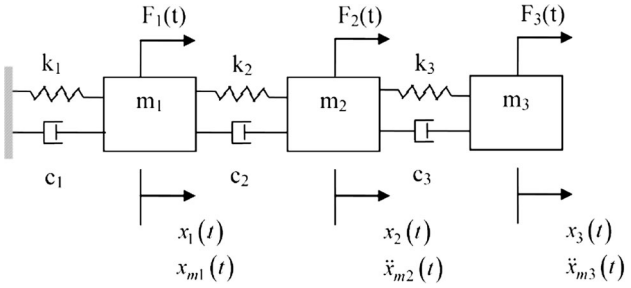

Fig. 5 Three degree of freedom spring–mass–dashpot system. Note that the first degree of freedom is associated with a nonlinear hysteretic component [25]

measurements for different DOFs is assumed. Three degree of freedom spring–mass–dashpot system is illustrated in Fig. 5, which is usually used in SHM literature for the performance evaluation of state estimation techniques. In the considered system, the first degree of freedom is associated with a nonlinear hysteretic component [25].

The system can be modeled by the equation of motion as follows:

$$M\ddot{x}(t) + C\dot{x}(t) + Rx(t) = F(t), \tag{41}$$

where M and C are the matrices of mass and damping, R is the restoring force, $x(t)$ is the vector of displacements, $\dot{x}(t)$ is the vector of velocities, $\ddot{x}(t)$ is the vector of accelerometer measurements and $F(t)$ is the vector of excitation force.

The restoring force R can be expressed as:

$$R = ak_i x(t) + (1-a)k_i r(t), \tag{42}$$

where $a = \frac{k_f}{k_i}$ is the ratio of post-yield k_f to pre-yield k_i stiffness and $r_1(k)$ is the Bouc–Wen hysteretic component that can be written as follows:

$$\dot{r}_1(k) = \dot{x}_1 - \beta|\dot{x}_1||r_1|^{n-1}r - \gamma(\dot{x}_1)|r_1|^n, \tag{43}$$

where β, γ and n are the Bouc–Wen hysteretic parameters.

The system can be represented by the following state equation:

$$\begin{bmatrix} x_1 \\ x_2 \\ x_3 \end{bmatrix} -> \begin{bmatrix} m_1 & 0 & 0 \\ 0 & m_2 & 0 \\ 0 & 0 & m_3 \end{bmatrix} \begin{bmatrix} \ddot{x}_1 \\ \ddot{x}_2 \\ \ddot{x}_3 \end{bmatrix} + \begin{bmatrix} c_1+c_2 & -c_2 & 0 \\ -c_2 & c_2+c_3 & -c_3 \\ 0 & -c_3 & c_3 \end{bmatrix}$$
$$\times \begin{bmatrix} \dot{x}_1 \\ \dot{x}_2 \\ \dot{x}_3 \end{bmatrix} + \begin{bmatrix} k_1 & k_2 & -k_3 & 0 \\ 0 & -k_2 & k_2+k_3 & -k_3 \\ 0 & 0 & -k_3 & k_3 \end{bmatrix} \begin{bmatrix} r_1 \\ x_1 \\ x_2 \\ x_3 \end{bmatrix} = \begin{bmatrix} F_1(k) \\ F_2(k) \\ F_3(k) \end{bmatrix} \tag{44}$$

where $r_1(k)$ is the Bouc–Wen hysteretic component with:

$$\dot{r}_1(k) = \dot{x}_1 - \beta|\dot{x}_1||r_1|^{n-1}r - \gamma(\dot{x}_1)|r_1|^n \tag{45}$$

β, γ and n are the Bouc–Wen hysteretic parameters.

The state and observation formulations are detailed in our previous work [1].

5.2.1 Generation of dynamic data

For dynamic data generation from the SHM system (46) [25] is used to simulate the responses of the state as functions of time by solving the differential Eq. (46) using fourth-order Runge–Kutta Integration.

$$\dot{y} = \begin{bmatrix} \dot{y}_1 \\ \dot{y}_2 \\ \dot{y}_3 \\ \dot{y}_4 \\ \dot{y}_5 \\ \dot{y}_6 \\ \dot{y}_7 \end{bmatrix} = \begin{bmatrix} \dot{x}_1 \\ \dot{x}_2 \\ \dot{x}_3 \\ \dot{r}_1 \\ \ddot{x}_1 \\ \ddot{x}_2 \\ \ddot{x}_3 \end{bmatrix}$$
$$= \begin{bmatrix} z_5 \\ z_6 \\ z_7 \\ z_5 - 2|z_5||z_4|^{2-1}z_4 - 1z_5|z_4|^2 \\ -9z_4 - 9z_1 + 9z_2 - 0.5z_5 + 0.25z_6 + \ddot{v}_g \\ -9z_1 - 18z_2 + 9z_3 - 0.25z_5 + 0.5z_6 + 0.25z_z - \ddot{v}_g \\ 9z_2 - 9z_3 + 0.25z_6 - 0.25z_7 - \ddot{v}_g \end{bmatrix}, \tag{46}$$

where the state variables x_1, x_2, x_3 are displacements and r_1 is the hysteretic Bouc–Wen parameter.

It must be noted that these simulated states are assumed to be noise free. They are contaminated with zero mean Gaussian errors. The SHM parameters as well as other physical properties are shown in Table 3. Figure 6 shows the changes in the state variable (displacement x_1).

Table 3 SHM parameters and physical properties

Parameter	Value	Parameter	Value	Parameter	Value
m_1	1	m_2	1	m_3	1
c_1	0.25	c_2	0.25	c_3	0.25
k_1	9	k_2	9	k_3	9
β	2	γ	1	n	2

For all simulations, the following parameters are used. The sampling frequency of the Northridge earthquake acceleration data that was used as ground excitation $\ddot{v}_g$, is 100 Hz ($T = 0.01$ s). The Northridge earthquake signal was filtered with a low-frequency cutoff of 0.13 Hz and a high-frequency cutoff of 30 Hz. A duration of 20 s of the earthquake record was adopted [25]. The number of sigma points is fixed to 32 for all the techniques ($L = 16$). The process noise of 1 % RMS noise-to-signal ratio was added. The observation noise level was of 4 % RMS noise-to-signal ratio. The initial values of the augmented state vector $z(0) = [x_0 \quad \theta_0]$ are given by:

$$x_0 = [0 \quad 0 \quad 0 \quad 0 \quad 0 \quad 0 \quad 0]\text{and}$$
$$\theta_0 = [6 \quad 6 \quad 6 \quad 0.5 \quad 0.5 \quad 0.5 \quad 3 \quad 2 \quad 1].$$

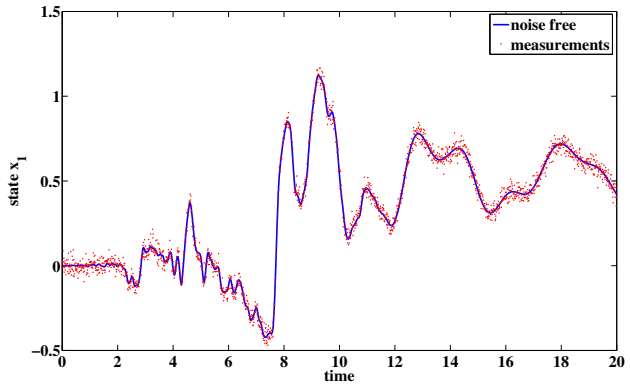

Fig. 6 Simulated data used in estimation: state variable (x_1)

5.2.2 *Comparative study 1: estimation of state variables from noisy measurements*

The purpose of this study is to compare the estimation accuracy of UKF, SRCDKF, IUKF, ISRCDKF, PF, UKF-PF, SRCDKF-PF, IUKF-PF and ISRCDKF-PF methods when they are utilized to estimate the seven state variables of the three degree of freedom spring–mass–dashpot system model. Hence, it is considered that the state vector to be estimated, $z_k = x_k = [x_1\ x_2\ x_3\ r_1\ v_1\ v_2\ v_3]^T$, and the model parameters, k_1, k_2, k_3, c_1, c_2, c_3, β, γ, and n are assumed to be known.

The simulation results for state estimations of seven state variables x_1, x_2, x_3, r_1, v_1, v_2 and v_3 using UKF, SRCDKF, IUKF, ISRCDKF, PF, UKF-PF, SRCDKF-PF, IUKF-PF and ISRCDKF-PF methods are shown in Figs. 7a–d, 8a–d, 9a–d and 10a–d, respectively. Also, the performance comparison of the state estimation techniques in terms of RMSE are presented in Table 4 (mean RMSE (MRMSE) for UKF=0.0328 , SRCDKF= 0.0326, IUKF= 0.0323, ISRCDKF= 0.0320,PF = 0.0326, MRMSE (UKF-PF) = 0.0313, MRMSE (SRCDKF-PF) = 0.0312, MRMSE (IUKF-PF) = 0.0307, and MRMSE (ISRCDKF-PF) = 0.0305. It is easily observed from Figs. 7, 8, 9a–d and 10a–d as well as Table 4 that PF is outperformed by the alternative techniques (see Table 4). The results also show that the ISRCDKF-PF method achieves a better accuracy than the IUKF-PF method. Both ISRCDKF-PF and IUKF-PF methods can provide improved accuracy over the UKF-PF and SRCDKF-PF approaches.

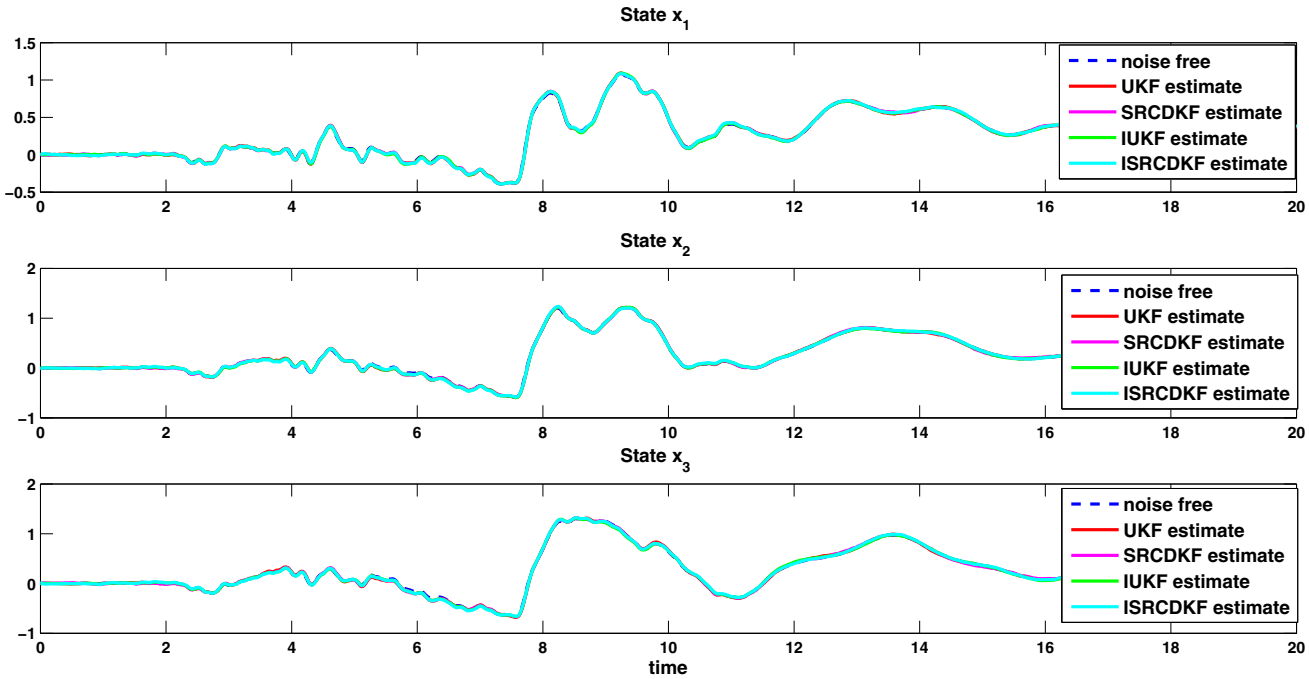

Fig. 7 Estimation of state variables using various state estimation techniques (UKF, IUKF, SRCDKF and ISRCDKF)

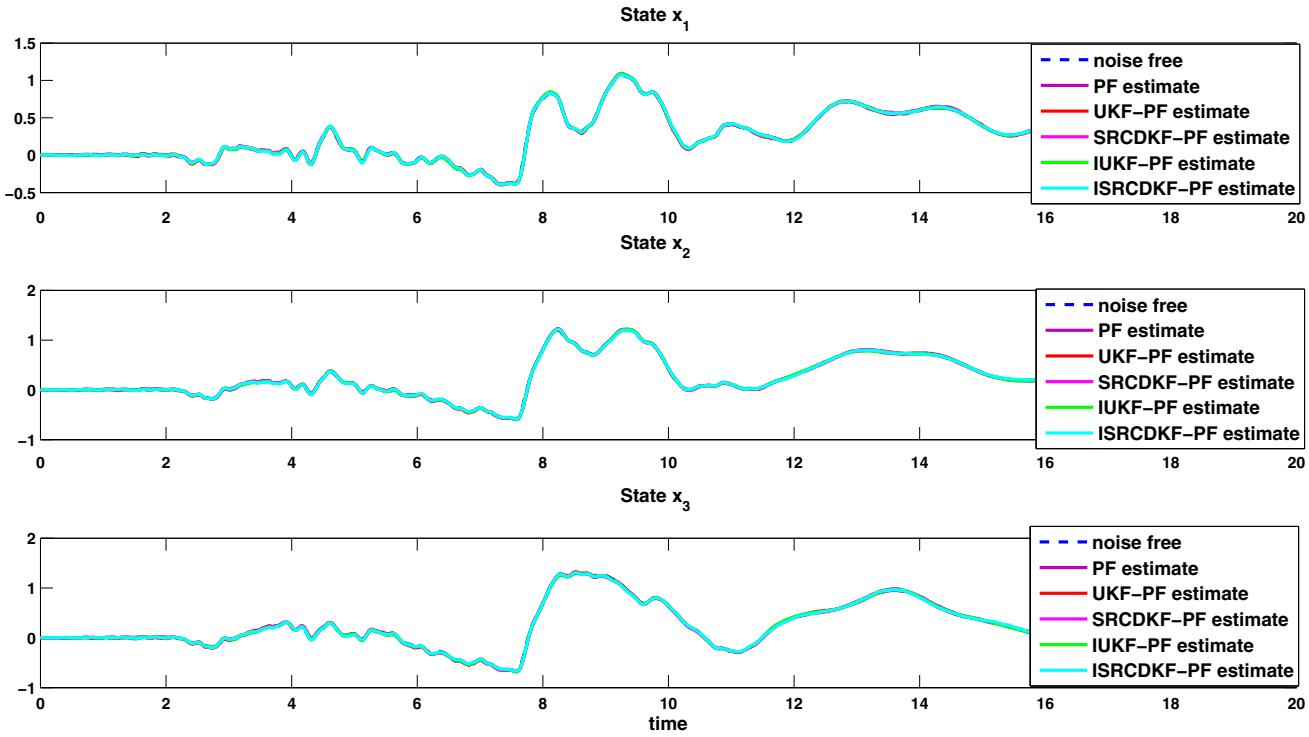

Fig. 8 Estimation of state variables using various state estimation techniques (PF, UKF-PF, IUKF-PF, SRCDKF-PF and ISRCDKF-PF)

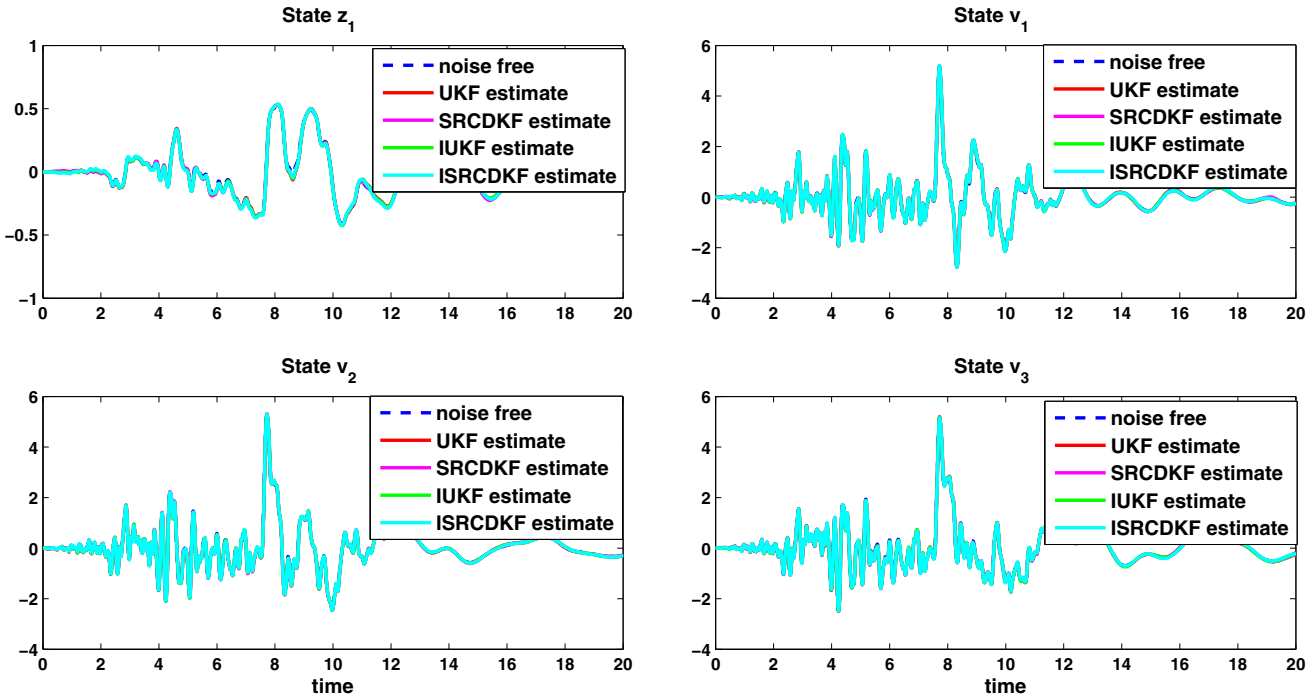

Fig. 9 Estimation of state variables using various state estimation techniques (UKF, IUKF, SRCDKF and ISRCDKF)

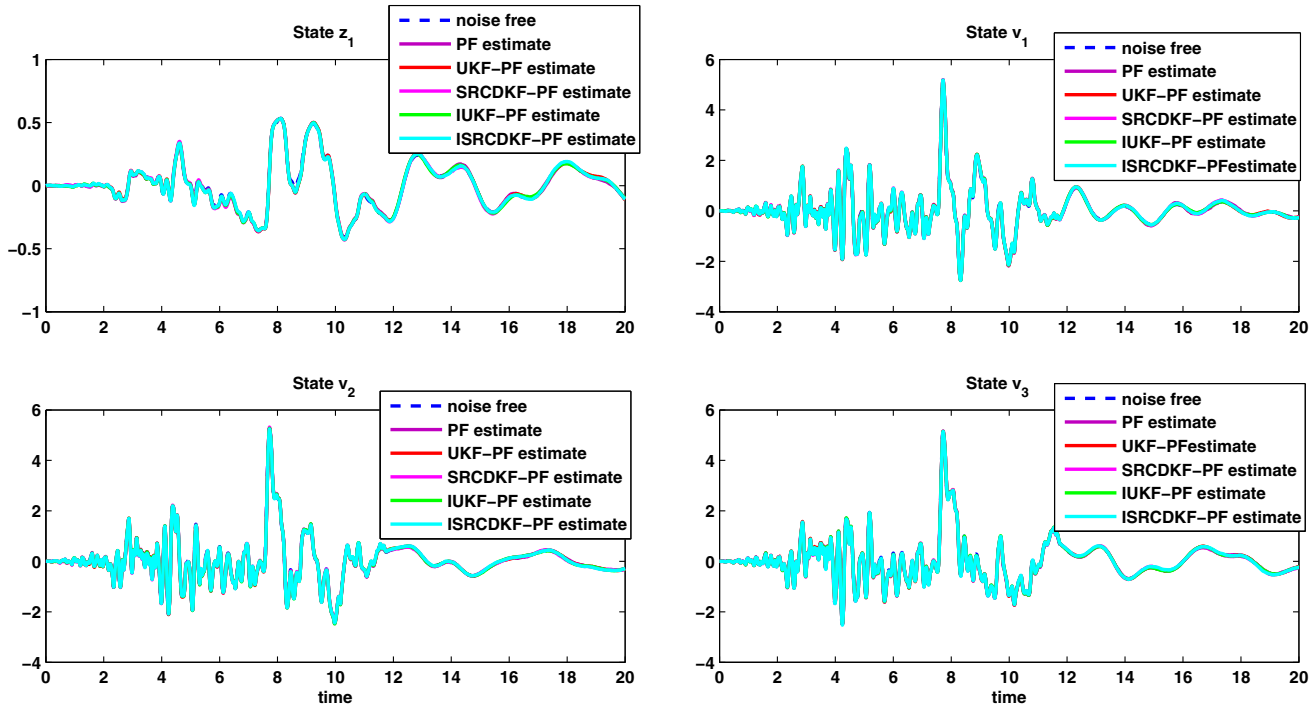

Fig. 10 Estimation of state variables using various state estimation techniques (PF, UKF-PF, IUKF-PF, SRCDKF-PF and ISRCDKF-PF)

Table 4 Comparison of state estimation techniques

Technique	x_1	x_2	x_3	r_1	v_1	v_2	v_3
UKF	0.0097	0.0124	0.0159	0.0117	0.0624	0.0593	0.0586
SRCDKF	0.0097	0.0123	0.0157	0.0114	0.0622	0.0589	0.0585
IUKF	0.0094	0.0122	0.0149	0.0111	0.0622	0.0583	0.0581
ISRCDKF	0.0093	0.0119	0.0147	0.0108	0.0620	0.0578	0.0576
PF	0.0096	0.0115	0.0141	0.0123	0.0654	0.0573	0.0585
UKF-PF	0.0091	0.0106	0.0129	0.0108	0.0614	0.0572	0.0573
SRCDKF-PF	0.0089	0.0105	0.0124	0.0109	0.0616	0.0573	0.0573
IUKF-PF	0.0087	0.0105	0.0123	0.0106	0.0610	0.0571	0.0556
ISRCDKF-PF	0.0081	0.0096	0.0123	0.0100	0.0609	0.0566	0.0554

5.2.3 *Comparative study 2: simultaneous estimation of state variables and model parameters*

The estimation of the state variables and parameters were performed using the state estimation techniques, UKF, SRCDKF, IUKF, ISRCDKF, PF, UKF-PF, SRCDKF-PF, IUKF-PF and ISRCDKF-PF. The estimation results for the model parameters using the estimation techniques (UKF, SRCDKF, IUKF, ISRCDKF, PF, UKF-PF, IUKF-PF, SRCDKF-PF and ISRCDKF-PF) are shown in Figs. 11, 12, 13, 14 , 15 and 16, respectively.

It can be seen from the results presented in Figs. 11, 12, 13, 14 , 15 and 16 that the UKF-PF, IUKF-PF and SRCDKF-PF methods outperform the PF ,ISRCDKF, IUKF, SRCDKF, and UKF methods, and that the ISRCDKF-PF shows relative improvement over all other techniques. These results confirm the results obtained in the first comparative study, where only the state variables are estimated. The advantages of the ISRCDKF-PF over the IUKF-PF (and the IUKF-PF over the PF, the UKF-PF and the SRCDKF-PF) can also be seen through their abilities to estimate the model parameters. For example, UKF, SRCDKF, IUKF, ISRCDKF, PF, UKF-PF, IUKF-PF and SRCDKF-PF could took longer to estimate a model parameters (see Figs. 11, 12, 13, 14, 15, 16). The ISRCDKF-PF, however, could estimate all the model parameters in all four cases.

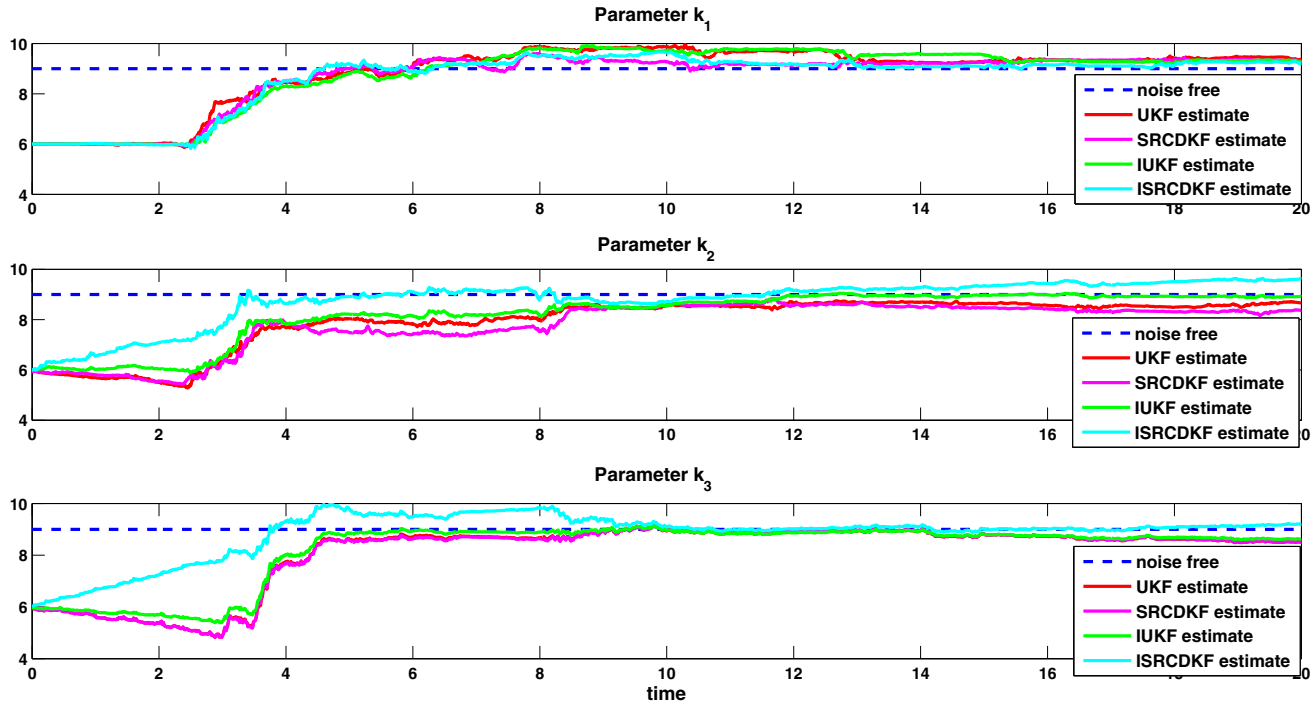

Fig. 11 Estimation of the model parameters (k_1, k_2 and k_3) using UKF, SRCDKF, IUKF and ISRCDKF

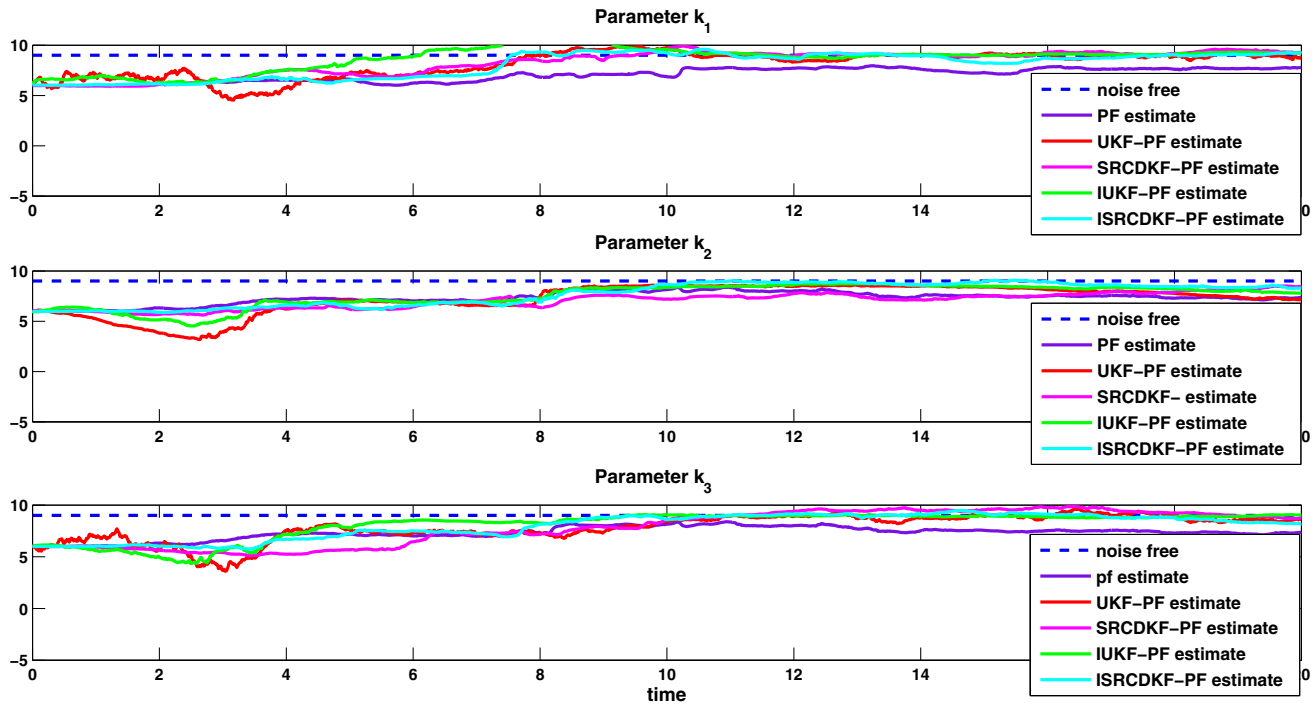

Fig. 12 Estimation of the model parameters (k_1, k_2 and k_3) using PF, UKF-PF, SRCDKF-PF, IUKF-PF and ISRCDKF-PF

5.2.4 Root mean square error analysis

Some practical challenges, however, can affect the accuracy of estimated states and/or parameters. Such challenges include the large number of states and parameters to be estimated, and the presence of measurement noise in the data. The effect of the these challenges on the performances of the UKF, IUKF, SRCDKF, ISRCDKF, PF,

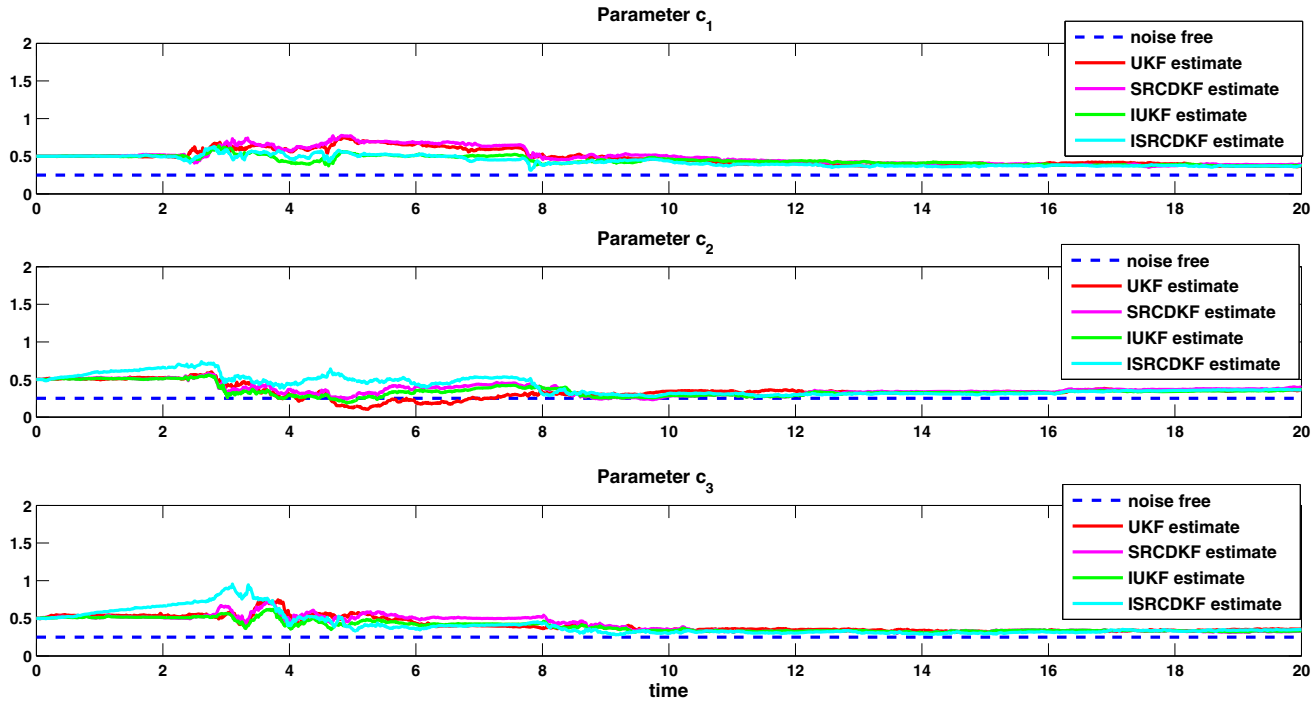

Fig. 13 Estimation of the model parameters (c_1, c_2 and c_3) using UKF, SRCDKF, IUKF and ISRCDKF

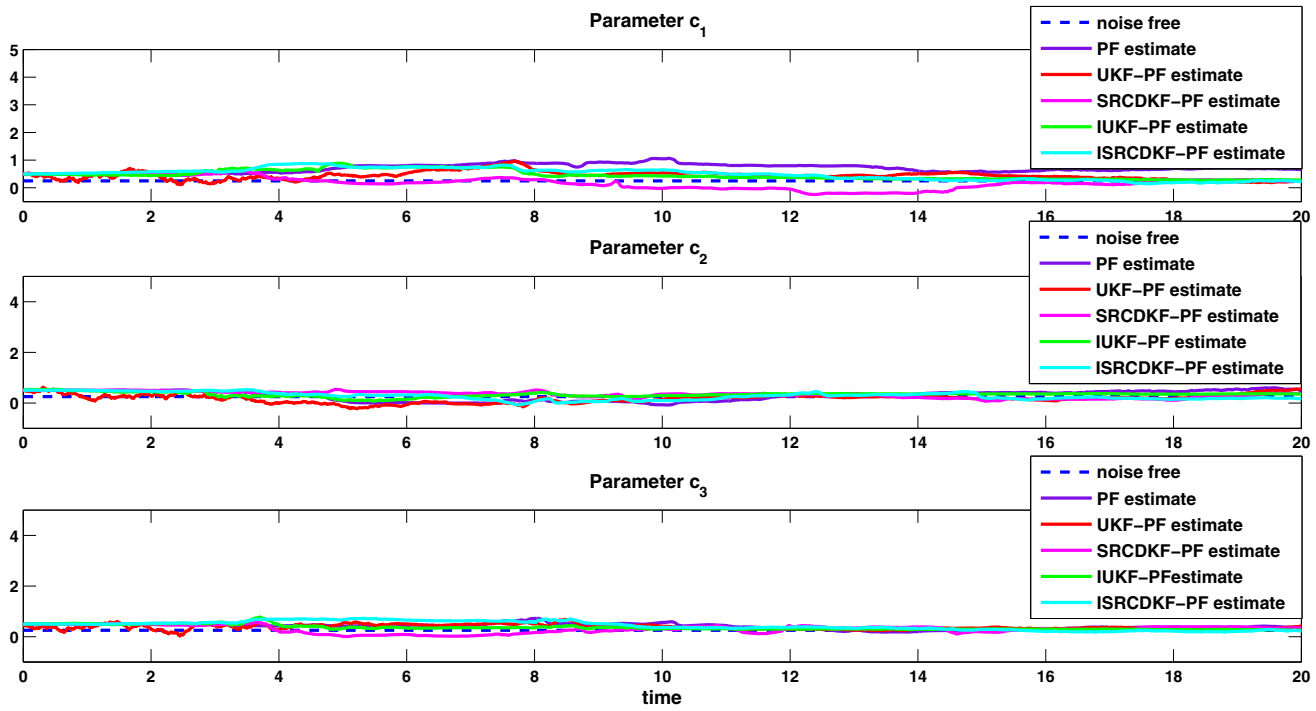

Fig. 14 Estimation of the model parameters (c_1, c_2 and c_3) using PF, UKF-PF, SRCDKF-PF, IUKF-PF and ISRCDKF-PF

UKF-PF, IUKF-PF, SRCDKF-PF and ISRCDKF-PF for state and parameter estimation are investigated.

(a) Effect of number of state and parameter to estimate on the estimation RMSE

To study the effect of the number of states and parameters to be estimated on the estimation performances of PF, UKF-PF, IUKF-PF, SRCDKF-PF and ISRCDKF-PF, the estimation is analyzed for different numbers of estimated

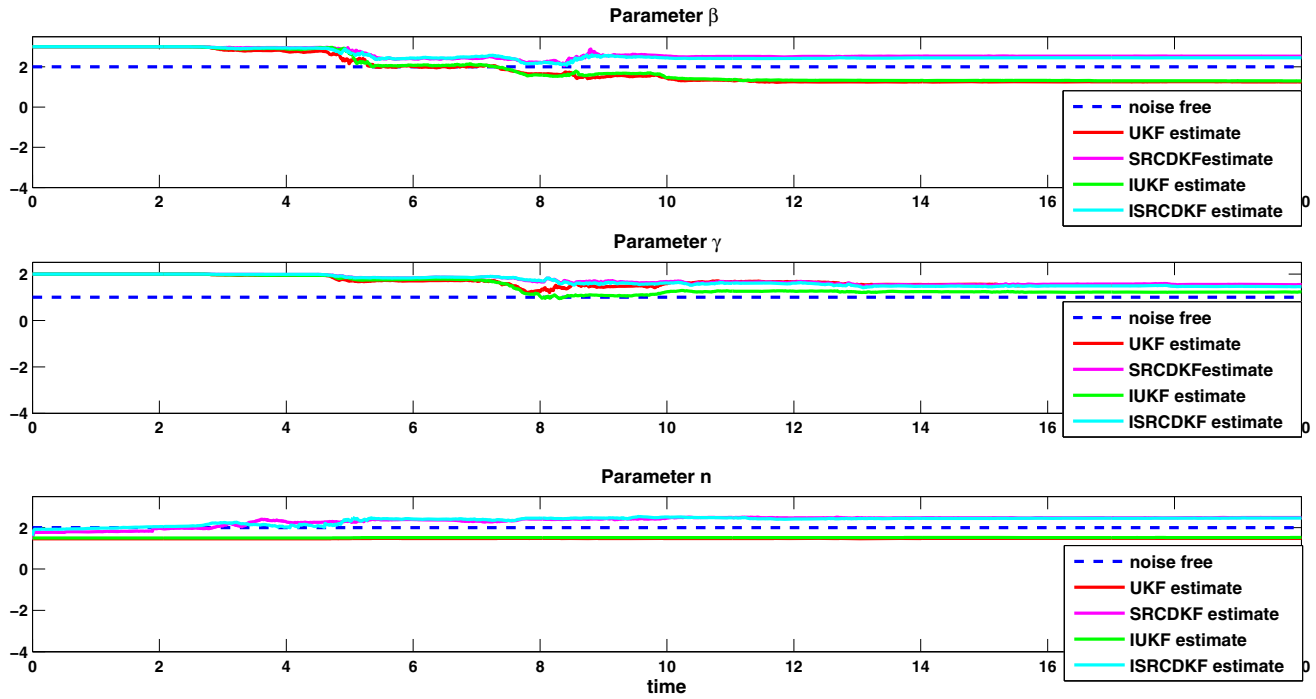

Fig. 15 Estimation of the model parameters (β, γ and n) using UKF, SRCDKF, IUKF and ISRCDKF

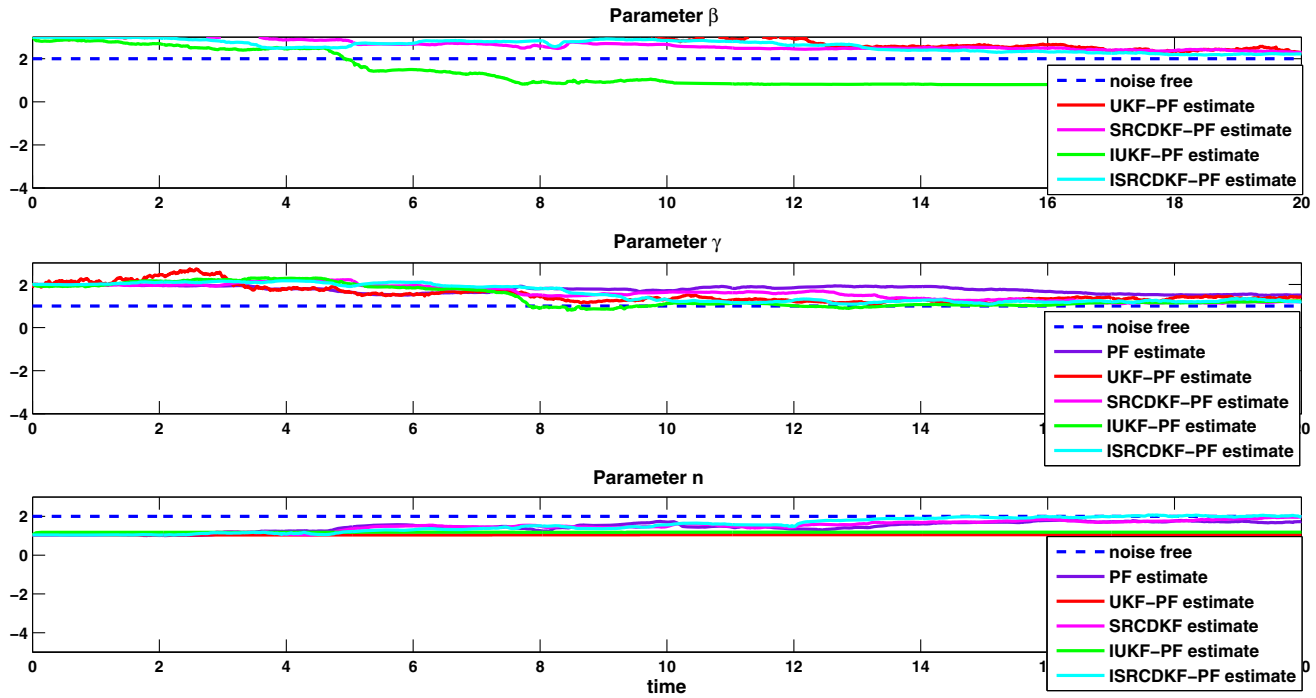

Fig. 16 Estimation of the model parameters (β, γ and n) using PF, UKF-PF, IUKF-PF, SRCDKF-PF and ISRCDKF-PF

states and parameters. Here, we will consider three cases, which are summarized below. In all cases, it is assumed that the seven states x_1, x_2, x_3, r_1, v_1, v_2 and v_3 are measured.

1. Case 1: the seven states x_1, x_2, x_3, r_1, v_1, v_2 and v_3 along with the first parameter k_1 will be estimated.
2. Case 2: the seven states $x_1, x_2, x_3, r_1, v_1, v_2$ and v_3 along with the two parameters k_1 and k_2 will be estimated.

Table 5 Root mean square errors of estimated state variables and mean of estimated parameter

Technique	x_1	x_2	x_3	r_1	v_1	v_2	v_3	k_1
UKF	0.0110	0.0127	0.0156	0.0153	0.0677	0.0601	0.0605	8.9610
SRCDKF	0.0110	0.0124	0.0152	0.0154	0.0679	0.0594	0.0593	8.9613
IUKF	0.0109	0.0123	0.0150	0.0147	0.0683	0.0589	0.0590	8.9725
ISRCDKF	0.0106	0.0119	0.0143	0.0154	0.0690	0.0579	0.0571	8.9741
PF	0.0119	0.0139	0.0164	0.0210	0.0760	0.0585	0.0577	8.8551
UKF-PF	0.0103	0.0117	0.0137	0.0160	0.0694	0.0558	0.0560	8.9372
SRCDKF-PF	0.0099	0.0114	0.0134	0.0155	0.0683	0.0559	0.0558	8.9459
IUKF-PF	0.0098	0.0112	0.0133	0.0150	0.0677	0.0552	0.0554	8.9520
ISRCDKF-PF	0.0096	0.0109	0.0130	0.0147	0.0671	0.0547	0.0546	8.9578

Table 6 Root mean square errors of estimated state variables and mean of estimated parameter

Technique	x_1	x_2	x_3	r_1	v_1	v_2	v_3	k_1	k_2
UKF	0.0106	0.0224	0.0310	0.0165	0.0739	0.0644	0.0668	8.8517	8.6560
SRCDKF	0.0106	0.0224	0.0308	0.0163	0.0738	0.0641	0.0670	8.8597	8.6936
IUKF	0.0105	0.0222	0.0302	0.0158	0.0753	0.0637	0.0665	8.8561	8.7339
ISRCDKF	0.0105	0.0220	0.0298	0.0155	0.0751	0.0632	0.0665	8.8728	8.7901
PF	0.0128	0.0267	0.0294	0.0180	0.0780	0.0671	0.0657	8.1775	8.3102
UKF-PF	0.0104	0.0217	0.0230	0.0147	0.0737	0.0638	0.0635	8.8825	8.7749
SRCDKF-PF	0.0103	0.0213	0.0229	0.0148	0.0731	0.0632	0.0629	8.8844	8.7909
IUKF-PF	0.0101	0.0196	0.0212	0.0142	0.0730	0.0610	0.0619	8.8880	8.826
ISRCDKF-PF	0.0101	0.0191	0.0205	0.0137	0.0727	0.0605	0.0614	8.9046	8.8166

3. Case 3: the seven states x_1, x_2, x_3, r_1, v_1, v_2 and v_3 along with all the model parameters k_1, k_2, k_3, c_1, c_2, c_3, β, γ, and n will be estimated. In case 3 where all the parameters are estimated, we have added constraint on the parameter n. In fact, in the spring–mass–dashpot system, the nonlinear spring is mathematically ill-defined for negative values of n and physically the values of n cannot be smaller than 1 [37]. So when generating the sigma points, if the value of n is smaller than 1, we shift the mean for the symmetric sigma points by the small amount as follows: $Z(16, i) = (1 + 0.5 * \text{rand}) *$ constraints.value (where i = number of sigma points and constraints.value = 1).

The estimation of the state variables and parameter(s) for these three cases is performed using UKF, SRCDKF, IUKF, ISRCDKF, PF, UKF-PF, IUKF-PF, SRCDKF-PF and ISRCDKF-PF, and the simulation results for the state variables and the model parameters for the three cases are shown in Tables 5, 6 and 7. For example, for case 1, Table 5 compares the estimation root mean square errors for the seven state variables x_1, x_2, x_3, r_1, v_1, v_2 and v_3 (with respect to the noise-free data) and the mean of the estimated parameter k_1 at steady state (i.e., after convergence of parameter(s)) using UKF, SRCDKF, IUKF, ISRCDKF, PF, UKF-PF, IUKF-PF, SRCDKF-PF and ISRCDKF-PF, respectively. Tables 6 and 7 also present similar comparisons for cases 2 and 3, respectively.

The results also show that the number of parameters to estimate affects the estimation accuracy of the state variables. In other words, for PF the estimation RMSE of x_1, x_2, x_3, r_1, v_1, v_2 and v_3 increases from the first comparative study (where only the state variables are estimated) to case 1 (where the states and one parameter, k_1, are estimated), case 2 (where the states and two parameters, k_1 and k_2, are estimated) to case 3 (where the states and nine parameters, k_1, k_2, k_3, c_1, c_2, c_3, β, γ, and n, are estimated). For example, the RMSEs obtained using PF for x_1 in the first comparative study and cases 1, 2, 3 of the second comparative study are 0.0096, 0.0119, 0.0128 and 0.0180, respectively, which increase as the number of estimated parameters increases (see Tables 5, 6, 7). This observation is valid for the other state variables x_2, x_3, z_1, v_1, v_2 and v_3 and for the other state estimation techniques UKF-PF, IUKF-PF, SRCDKF-PF and ISRCDKF-PF.

In Fig. 15, the initial value of the parameter n has automatically been changed in all the filters as the UKF, SRCDKF, IUKF et ISRCDKF. This change is due to the constraint applied on that parameter n because it value should not be smaller than 1.

It can also be shown from Tables 5, 6 and 7 that, for all the techniques, estimating more model parameters affects

Table 7 Root mean square errors of estimated state variables and mean of estimated parameter

Technique	x_1	x_2	x_3	r_1	v_1	v_2	v_3
UKF	0.0160	0.0339	0.0448	0.0336	0.0870	0.0679	0.0831
SRCDKF	0.0161	0.0338	0.0449	0.0332	0.0869	0.0678	0.0827
IUKF	0.0163	0.0334	0.0441	0.0327	0.0867	0.0676	0.0825
ISRCDKF	0.0165	0.0330	0.0436	0.0325	0.0865	0.0671	0.0822
PF	0.0180	0.0490	0.0520	0.0257	0.1034	0.0797	0.0864
UKF-PF	0.0165	0.0323	0.0425	0.0321	0.0861	0.0662	0.0823
SRCDKF-PF	0.0165	0.0317	0.0420	0.0313	0.0854	0.0656	0.0826
IUKF-PF	0.0164	0.0305	0.0422	0.0320	0.0856	0.0659	0.0820
ISRCDKF-PF	0.0162	0.0297	0.0413	0.0309	0.0847	0.0664	0.0815

Technique	k_1	k_2	k_3	c_1	c_2	c_3	β	γ	n
UKF	9.3364	8.5977	8.6950	0.3913	0.3420	0.3382	1.2551	1.5088	1.4744
SRCDKF	9.2671	8.4281	8.7637	0.3902	0.3388	0.3301	2.5260	1.5754	2.2117
IUKF	9.3818	9.0316	8.7422	0.3899	0.3354	0.3304	1.3093	1.2214	1.5188
ISRCDKF	9.1402	9.4149	9.2875	0.3711	0.3339	0.3219	2.4496	1.4780	2.1592
PF	7.3935	7.5139	8.0480	0.6431	0.3553	0.3253	2.8813	1.7200	1.6164
UKF-PF	8.9639	8.2504	8.8166	0.3653	0.2807	0.3148	2.4384	1.3653	1.525
SRCDKF-PF	8.8793	8.8175	8.7905	0.3108	0.2521	0.3194	2.4529	1.2996	1.8357
IUKF-PF	9.1030	8.8322	8.8760	0.3063	0.2576	0.2876	2.4384	1.1594	1.1828
ISRCDKF-PF	8.8803	8.8410	8.8751	0.2594	0.2515	0.2520	2.2359	1.2301	1.9682

Table 8 Root mean square errors (RMSE) of the estimated states using PF for different noise levels

Noise levels	x_1	x_2	x_3	r_1	v_1	v_2	v_3
10^{-1}	0.0125	0.0259	0.0371	0.0356	0.1066	0.0797	0.0951
10^{-2}	0.0096	0.0115	0.0141	0.0123	0.0654	0.0573	0.0585
10^{-3}	0.0093	0.0099	0.0129	0.0107	0.0652	0.0560	0.0553

Table 9 Root mean square errors (RMSE) of the estimated states using UKF-PF for different noise levels

Noise levels	x_1	x_2	x_3	r_1	v_1	v_2	v_3
10^{-1}	0.0109	0.0133	0.0166	0.0129	0.0645	0.0622	0.0620
10^{-2}	0.0091	0.0106	0.0129	0.0108	0.0614	0.0572	0.0573
10^{-3}	0.0087	0.0101	0.0117	0.0102	0.0584	0.0522	0.0524

the estimation accuracy. The ISRCDKF-PF method, however, still provides advantages over other methods in terms of the estimation accuracy. These advantages of the ISRCDKF-PF are due to the fact that it uses a better proposal distribution that takes the latest observation into account by using ISRCDKF.

It can also be shown from Tables 5, 6 and 7 that, for all the techniques, estimating more model parameters affects the estimation accuracy. The ISRCDKF-PF method, however, still provides advantages over other methods in terms of the estimation accuracy. These advantages of the ISRCDKF-PF are due to the fact that it uses a better proposal distribution that takes the latest observation into account by using ISRCDKF.

(b) Effect of noise content on the estimation RMSE

It is assumed that a noise is added to the state variables. In order to show the performance of PF, UKF-PF, IUKF-PF, SRCDKF-PF and ISRCDKF-PF estimation algorithms in the presence of noise, three different measurements noise values, 10^{-1}, 10^{-2} and 10^{-3} are considered. The simulation results of estimating the seven states x_1, x_2, x_3, r_1, v_1, v_2 and v_3 using PF, UKF-PF, IUKF-PF, SRCDKF-PF and ISRCDKF-PF methods when the noise levels vary in $\{10^{-1}$, 10^{-2} and $10^{-3}\}$ are shown in Tables 8, 9, 11, 10 and 12.

Table 10 Root mean square errors (RMSE) of the estimated states using SRCDKF-PF for different noise levels

Noise levels	x_1	x_2	x_3	r_1	v_1	v_2	v_3
10^{-1}	0.0108	0.0129	0.0157	0.0128	0.0639	0.0624	0.0623
10^{-2}	0.0089	0.0105	0.0124	0.0109	0.0616	0.0573	0.0573
10^{-3}	0.0084	0.0098	0.0103	0.0100	0.0544	0.0536	0.0534

Table 11 Root mean square errors (RMSE) of the estimated states using IUKF-PF for different noise levels

Noise levels	x_1	x_2	x_3	r_1	v_1	v_2	v_3
10^{-1}	0.0097	0.0119	0.0146	0.0124	0.0620	0.0583	0.0582
10^{-2}	0.0087	0.0105	0.0123	0.0106	0.0610	0.0571	0.0556
10^{-3}	0.0081	0.0096	0.0098	0.0100	0.0538	0.0535	0.0532

Table 12 Root mean square errors (RMSE) of the estimated states using ISRCDKF-PF for different noise levels

Noise levels	x_1	x_2	x_3	r_1	v_1	v_2	v_3
10^{-1}	0.0097	0.0116	0.0139	0.0120	0.0614	0.0575	0.0578
10^{-2}	0.0081	0.0096	0.0123	0.0100	0.0609	0.0566	0.0554
10^{-3}	0.0077	0.0092	0.0099	0.0095	0.0528	0.0533	0.0530

In other words, for the PF, UKF-PF, IUKF-PF, SRCDKF-PF and ISRCDKF-PF estimation techniques, the estimation RMSEs of x_1, x_2, x_3, r_1, v_1, v_2 and v_3 increase from the first comparative study (noise variance = 10^{-1}) to case (where the noise value = 10^{-4}). For example, the RMSEs obtained using PF for x_1 where the noise level in $\{10^{-1}, 10^{-2}$ and $10^{-3}\}$ are 0.0125, 0.0096 and 0.0093, which increase as the noise variance increases (refer to Tables 8, 9, 11, 10, 12). This observation is valid for the other state variables x_2, x_3, r_1, v_1, v_2 and v_3 and for the UKF-PF, IUKF-PF, SRCDKF-PF and ISRCDKF-PF algorithms.

The results of the ISRCDKF-PF are consistent for different state and/or parameter initial conditions. This is because, unlike other optimization techniques (which can easily converge at a local minima), the ISRCDKF-PF is a Monte Carlo-based technique which searches for the optimum solution of the state and/or parameter by generating a large number of samples that are used to approximate the posterior density function. These randomly generated samples that are used to approximate the posterior are independent of the initial conditions, making the ISRCDKF-PF robust to the choice of any initial conditions.

6 Conclusions

In this paper, the problem of state and parameter estimations of structural systems were addressed using the developed iterated square-root central difference Kalman particle filter (ISRCDKF-PF). Various conventional and state-of-the-art state estimation methods are compared for the estimation performance (the unscented Kalman filter (UKF), the square-root central difference Kalman filter (SRCDKF), the iterated unscented Kalman filter (IUKF), the iterated square-root central difference Kalman filter (SRCDKF), the conventional particle filter (PF), the unscented Kalman particle filter (UKF-PF), the square-root central difference Kalman particle filter (SRCDKF-PF), the iterated unscented Kalman particle filter (IUKF-PF) and the developed ISRCDKF-PF) in two comparative studies. In the first comparative study, the displacements and the velocities state variables are estimated from noisy measurements of these variables, and the various estimation techniques are compared by computing the estimation root mean square error with respect to the noise-free data. In the second comparative study, the state variables as well as the model parameters are simultaneously estimated. In this case, in addition to comparing the performances of the various state estimation techniques, the effect of the number of estimated model parameters on the accuracy and convergence of these techniques is also assessed. The results of the second comparative study show that, for all the techniques, estimating more model parameters affects the estimation accuracy as well as the convergence of the estimated states and parameters. The developed ISRCDKF-PF method, however, still provides advantages over other methods in terms of the estimation accuracy and convergence.

Acknowledgments This work was made possible by NPRP Grant NPRP7-1172-2-439 from the Qatar National Research Fund (a member of Qatar Foundation). The statements made herein are solely the responsibility of the authors.

References

1. Mansouri M, Avci O, Nounou H, Nounou M (2015) Iterated square root unscented Kalman filter for nonlinear states and parameters estimation: three DOF damped system. J Civil Struct Health Monit 5(4):493–508
2. Mottershead JE, Foster CD (1991) On the treatment of ill-conditioning in spatial parameter estimation from measured vibration data. Mech Syst Signal Process 5(2):139–154
3. Sanayei M, McClain JA, Wadia-Fascetti S, Santini EM (1999) Parameter estimation incorporating modal data and boundary conditions. J Struct Eng 125(9):1048–1055
4. Beck JL, Katafygiotis LS (1998) Updating models and their uncertainties. I: Bayesian statistical framework. J Eng Mech 124(4):455–461
5. Katafygiotis LS, Beck JL (1998) Updating models and their uncertainties. II. Model identifiability. J Eng Mech 124(4):463–467
6. Vanik MW, Beck J, Au S (2000) Bayesian probabilistic approach to structural health monitoring. J Eng Mech 126(7):738–745
7. Avci O, Setareh M, Murray TM (2005) Effects of bottom chord extensions on the static and dynamic performance of steel joist supported floors. Ph.D. dissertation, University Libraries, Virginia Polytechnic Institute and State University
8. Au S-K (2012) Fast bayesian ambient modal identification in the frequency domain, part II. Posterior uncertainty. Mech Syst Signal Process 26:76–90
9. Du H, Zhang N, Samali B, Naghdy F (2012) Robust sampled-data control of structures subject to parameter uncertainties and actuator saturation. Eng Struct 36:39–48
10. Mao Z, Todd M (2013) Statistical modeling of frequency response function estimation for uncertainty quantification. Mech Syst Signal Process 38(2):333–345
11. Goulet JA, Smith IF (2012) Predicting the usefulness of monitoring for identifying the behavior of structures. J Struct Eng 139(10):1716–1727
12. Au S-K (2014) Uncertainty law in ambient modal identification—Part I. Theory. Mech Syst Signal Process 48(1):15–33
13. Erdogan YS, Catbas FN, Bakir PG (2014) Structural identification (St-id) using finite element models for optimum sensor configuration and uncertainty quantification. Finite Element Anal Des 81:1–13
14. Zhang Y, Yang W (2013) Bayesian strain modal analysis under ambient vibration and damage identification using distributed fiber bragg grating sensors. Sens Actuators A Phys 201:434–449
15. Ching J, Beck J (2004) Bayesian analysis of the Phase II IASC-ASCE structural health monitoring experimental benchmark data. J Eng Mech 130(10):1233–1244
16. Kuok SC, Yuen KV (2012) Structural health monitoring of canton tower using bayesian framework. Smart Struct Syst 10(4-5):375–391
17. Chen T, Morris J, Martin E (2005) Particle filters for state and parameter estimation in batch processes. J Process Control 15(6):665–673
18. Rabiei M, Modarres M (2013) A recursive bayesian framework for structural health management using online monitoring and periodic inspections. Reliab Eng Syst Saf 112:154–164
19. Rabiei M, Modarres M (2013) Quantitative methods for structural health management using in situ acoustic emission monitoring. Int J Fatigue 49:81–89
20. Flynn EB, Todd MD (2010) A bayesian approach to optimal sensor placement for structural health monitoring with application to active sensing. Mech Syst Signal Process 24(4):891–903
21. Zhu B, Frangopol DM (2013) Reliability assessment of ship structures using bayesian updating. Eng Struct 56:1836–1847
22. Beck JL, Yuen K-V (2004) Model selection using response measurements: Bayesian probabilistic approach. J Eng Mech 130(2):192–203
23. Lam HF, Ng CT (2008) The selection of pattern features for structural damage detection using an extended bayesian ANN algorithm. Eng Struct 30(10):2762–2770
24. Chatzi EN, Smyth AW (2009) The unscented Kalman filter and particle filter methods for nonlinear structural system identification with non-collocated heterogeneous sensing. Struct Control Health Monit 16(1):99–123
25. Chatzi EN, Smyth AW (2013) Particle filter scheme with mutation for the estimation of time-invariant parameters in structural health monitoring applications. Struct Control Health Monit 20(7):1081–1095
26. Kalman RE (1960) A new approach to linear filtering and prediction problem. Trans ASME Ser D J Basic Eng 82:34–45
27. Aidala V (1977) Parameter estimation via the Kalman filter. IEEE Trans Auto Control 22(3):471–472
28. Grewal MS, Andrews AP (2008) Kalman filtering: theory and practice using MATLAB. Wiley
29. Wan EA, Van Der Merwe R (2000) The unscented kalman filter for nonlinear estimation. In: Adaptive systems for signal processing, communications, and control symposium, AS-SPCC, The IEEE 2000, pp 153–158
30. Mansouri MM, Nounou HN, Nounou MN, Datta AA (2014) State and parameter estimation for nonlinear biological phenomena modeled by s-systems. Digit Signal Proc 28:1–17
31. Zhu J, Zheng N, Yuan Z, Zhang Q, Zhang X, He Y (2009) A slam algorithm based on the central difference Kalman filter. In: Intelligent vehicles symposium, 2009 IEEE, pp 123–128
32. Van Der Merwe R, Wan EA (2001) The square-root unscented Kalman filter for state and parameter-estimation. In: Acoustics, speech, and signal processing, 2001, Proceedings (ICASSP'01), 2001 IEEE International Conference on, vol 6, pp 3461–3464
33. NøRgaard M, Poulsen NK, Ravn O (2000) New developments in state estimation for nonlinear systems. Automatica 36(11):1627–1638
34. Zhan R, Wan J (2007) Iterated unscented kalman filter for passive target tracking. Aerosp Electron Syst IEEE Trans 43(3):1155–1163
35. Mariani S, Ghisi A (2006) Unscented Kalman filtering for nonlinear structural dynamics
36. Mu W, Smyth AW (2007) Application of the unscented Kalman filter for real-time nonlinear structural system identification. Struct Control Health Monit 14:971–990
37. Chatzi EN, Smyth AW (2009) The unscented kalman filter and particle filter methods for nonlinear structural system identification with non-collocated heterogeneous sensing. Struct Control Health Monit 16(1):99–123
38. Kotecha J, Djuric P (2003) Gaussian particle filtering. IEEE Trans Signal Process 51(10):2592–2601
39. Poyiadjis G, Doucet A, Singh S (2005) Maximum likelihood parameter estimation in general state-space models using particle methods. Proc Am Stat Assoc
40. Mansouri M, Snoussi H, Richard C (2009) A nonlinear estimation for target tracking in wireless sensor networks using quantized variational filtering. In: Signals, circuits and systems (SCS), 2009 3rd international conference on, IEEE 2009, pp 1–4
41. Doucet A, Tadić V (2003) Parameter estimation in general state-space models using particle methods. Ann Inst Stat Math 55(2):409–422
42. Arulampalam M, Maskell S, Gordon N, Clapp T (2002) A tutorial on particle filters for online nonlinear/non-gaussian bayesian tracking. Signal Process IEEE Trans 50(2):174–188
43. Haug A (2005) A tutorial on bayesian estimation and tracking techniques applicable to nonlinear and non-gaussian processes. MITRE Corporation, McLean

44. Mansouri M, Dumont B, Leemans V, Destain M-F (2014) Bayesian methods for predicting LAI and soil water content. Precision Agricult 15(2):184–201
45. Van Der Merwe R, Doucet A, De Freitas N, Wan E (2001) The unscented particle filter. Adv Neural Inf Process Syst pp 584–590
46. Liang-Qun L, Hong-Bing J, Jun-Hui L (2005) The iterated extended kalman particle filter. In: Communications and information technology, 2005, ISCIT 2005, IEEE international symposium on, vol 2, pp 1213–1216
47. Wu P, Li X, Bo Y (2013) Iterated square root unscented kalman filter for maneuvering target tracking using TDOA measurements. Int J Control Autom Syst 11(4):761–767
48. Gustafsson F, Gunnarsson F, Bergman N, Forssell U, Jansson J, Karlsson R, Nordlund P (2002) Particle filters for positioning, navigation, and tracking. Signal Process IEEE Trans 50(2):425–437
49. Doucet A, Johansen A (2009) A tutorial on particle filtering and smoothing: fifteen years later. In: Crisan D, Rozovsky B (eds) Handbook of nonlinear filtering. Oxford University Press, Oxford
50. Liu J, Chen R (1998) Sequential monte carlo methods for dynamic systems. J Am Stat Assoc 99(443):1032–1044